

Transport properties of a superconducting single-electron transistor coupled to a nanomechanical oscillator

V. Koerting,¹ T. L. Schmidt,¹ C. B. Doiron,¹ B. Trauzettel,² and C. Bruder¹

¹Department of Physics, University of Basel, CH-4056 Basel, Switzerland

²Institute for Theoretical Physics and Astrophysics,
University of Würzburg, D-97074 Würzburg, Germany

(Dated: February 21, 2024)

We investigate a superconducting single-electron transistor capacitively coupled to a nanomechanical oscillator and focus on the double Josephson quasiparticle resonance. The existence of two coherent Cooper pair tunneling events is shown to lead to pronounced backaction effects. Measuring the current and the shot noise provides a direct way of gaining information on the state of the oscillator. In addition to an analytical discussion of the linear-response regime, we discuss and compare results of higher-order approximation schemes and a fully numerical solution. We find that cooling of the mechanical resonator is possible, and that there are driven and bistable oscillator states at low couplings. Finally, we also discuss the frequency dependence of the charge noise and the current noise of the superconducting single electron transistor.

PACS numbers: 85.85.+j, 73.23.Hk, 73.50.Td

I. INTRODUCTION

The cooling of nanomechanical systems by measurement has received a lot of attention recently. Various procedures like the laser sideband cooling schemes developed for trapped ions and atoms,¹ have been proposed as ways to significantly cool a nanomechanical resonator (NR) coupled to a Cooper-pairbox,^{2,3,4,5} a flux qubit,^{6,7} quantum dots,¹¹ trapped ions,¹² and optical cavities.^{13,14,15,16,17,18,19,20,21,22,23,24,25,26,27,28,29,30,31,32,33,34} On the experimental side, optomechanical cooling schemes have been shown to be promising.^{13,14,15,16,17,18,19,20} the NR was cooled to ultra-low temperatures via either photothermal forces or radiation pressure by coupling it to a driven cavity.

Another important nanoelectromechanical measurement device which both holds the possibility of very accurate position measurements³⁵ as well as of cooling of an NR, is a superconducting single-electron transistor (SSET). Shortly after the theoretical proposals predicting the potential of the SSET to cool a nanomechanical system,^{8,9,67} this effect has been experimentally observed.¹⁰ Using other detectors for NRs such as normal-state single-electron transistors³⁶ or tunnel junctions,^{37,68} it is very difficult to cool the nanomechanical system or drive it into a non-classical state. These detectors usually act as heat baths with effective temperatures proportional to the transport voltage, which is in practice higher than the bath temperature. The SSET system, on the other hand, shows sharp transport resonances. At those the effective temperature is voltage-independent and can be made very low.

To achieve such challenging goals as ground-state cooling of NRs,¹⁰ or the creation of squeezed oscillator states, a better understanding of the transport properties of the coupled SSET-NR system is required. This system is schematically shown in Fig. 1. Depending on external pa-

rameters such as the gate voltage V_G , the bias voltage V , and also the superconducting gap Δ , the SSET supports different types of resonance conditions. The two most prominent ones are the so-called Josephson quasiparticle (JQP) and the double Josephson quasiparticle (DJQP) cycle.^{38,39} Whereas the former involves the coherent tunneling of a Cooper pair at one of the two junctions followed by a successive tunneling of two quasiparticles at the other junction, the latter consists of four steps (illustrated in Fig. 2 below) that involve a Cooper pair tunneling at each of the junctions and a quasiparticle tunneling at each of the junctions. The transport properties of the SSET coupled to an NR close to the JQP resonance have been analyzed in a recent theoretical work.⁴⁰ Here, we focus on the analysis of the same coupled quantum system at the DJQP resonance. Since the JQP is a one-dimensional resonance in the parameter space spanned by V_G and V and the DJQP is a zero-dimensional resonance in the same parameter space, all action and backaction effects close to the DJQP resonance are much more pronounced than close to the JQP resonance. This is of crucial importance if one wants to manipulate the state of the NR by measurement of the SSET detector because, in experiments, the typical coupling between the two quantum systems turns out to be rather weak.

We analyze how the NR can be cooled below the temperature of the external heat bath and how it can be brought into a (non-thermal) driven state at the DJQP resonance. Under certain conditions, we find signatures of bistable solutions of the coupled quantum system of NR and SSET. It is of particular interest and experimental relevance, to know how a successful cooling of the NR or the preparation of a driven state can be observed in transport properties of the SSET such as its current or current noise. We show that there is a one-to-one correspondence between interesting state preparations of the NR and the transport properties of the SSET. This provides a powerful and feasible tool to initialize and ma-

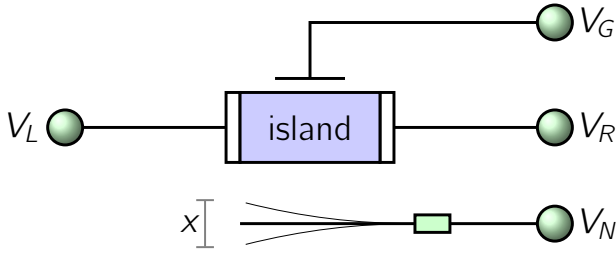


FIG. 1: Schematic setup of the SSET-resonator system: Two superconducting leads at voltages V_L and V_R are coupled by tunnel junctions to a superconducting island. Its chemical potential can be tuned by a gate voltage V_G . A nearby nanomechanical oscillator acts as an x -dependent gate.

nipulate NR quantum states by measurement.

The article is organized as follows. In section II, we present the model for the coupled quantum system of NR and SSET, discuss the different approximation schemes of the analytical solutions as well as the calculation scheme behind the exact numerical solution of the underlying master equation. Then, in section III, we analyze the oscillator properties by means of the different methods, identifying interesting quantum states of the NR due to its coupling to the SSET. Subsequently, in section IV, we discuss the current of the SSET detector and, in section V, the charge and current noise. It turns out that the combination of the two transport properties is sufficient to clearly identify a successful cooling or driven-state preparation of the oscillator. Finally, we present our conclusions in section VI. Details of the calculations are contained in the Appendices.

II. MODEL

The system under investigation consists of a superconducting single-electron transistor (SSET) which is capacitively coupled to a nanomechanical resonator (NR) as shown schematically in Fig. 1. The total Hamiltonian of the system reads

$$H = H_L + H_R + H_I + H_T + H_C + H_N + H_{N,I} : \quad (1)$$

The first three terms $H_{L,R,I}$ are standard BCS Hamiltonians and describe two superconducting leads (left and right) and a superconducting island,

$$H = \sum_{k;\uparrow} c_k^\dagger c_k + \sum_{k;\downarrow} c_k^\dagger c_k : \quad (2)$$

Here, c_k are annihilation operators for quasiparticles of momentum k and spin \uparrow in the system ($\uparrow = L, R, I$). The dispersion relation ϵ_k accounts for the superconducting gap of width 2Δ which we assume to be equal for the three systems. The chemical potentials in the left and right leads are determined by the applied bias voltage $V = V_L - V_R$, while the island chemical potential can be tuned by applying a gate voltage V_G (see Fig. 1).

The left and right leads are connected to the central island by quasiparticle tunneling and Cooper pair tunneling. Denoting by ϕ the superconducting phase difference at the junction $\uparrow = L, R$, we use the following quasiparticle tunneling term

$$H_{T,qp} = \sum_{\uparrow=L,R} \sum_{k;q;\downarrow} e^{i\phi_{\uparrow}} T_{kq} c_{k\downarrow}^\dagger c_{Iq} + \text{h.c.}; \quad (3)$$

where T_{kq} are the tunneling amplitudes which can be used to calculate⁴¹ the quasiparticle tunneling rates $\Gamma_{L,R}$. Cooper pair tunneling is accounted for by the term

$$H_{T,CP} = \sum_{\uparrow=L,R} J_{\uparrow} \cos \phi_{\uparrow}; \quad (4)$$

where J_{\uparrow} are the Josephson energies of the two junctions. Hence, the total tunneling Hamiltonian is given by $H_T = H_{T,qp} + H_{T,CP}$.

The final ingredient for the SSET Hamiltonian is the Coulomb energy of the island. If we denote by n_L and n_R the number of electrons that have tunneled from the island to the left and right lead, respectively, then $n = n_L - n_R$ is the excess number of electrons on the island. The charging term can be written as

$$H_C = E_C (n + n_0)^2 + eV n_R; \quad (5)$$

where E_C is the charging energy and n_0 can be controlled by the gate voltage (see Appendix A). In terms of the capacitances of the two junctions $C_{L,R}$, the gate C_G and the resonator C_N , the charging energy is given by $E_C = e^2/(2C)$, where $C = C_L + C_R + C_G + C_N$ is the total capacitance.

Next, we focus on the coupling of the SSET to the NR. The latter can be regarded as a harmonic oscillator of frequency ω and mass M and is therefore described by the Hamiltonian

$$H_N = \frac{p^2}{2M} + \frac{1}{2} M \omega^2 x^2 : \quad (6)$$

The NR is held on a constant voltage V_N and hence acts on the SSET as an additional gate with an x -dependent capacitance $C_N(x)$. Therefore, the presence of the NR modifies the charging term H_C . Expanding the contribution for small displacements x and retaining only the lowest order, one finds that the coupling between SSET and NR is given by

$$H_{N,I} = A n x; \quad (7)$$

where the coupling constant A depends in a non-trivial way on the voltages and capacitances of the system and can be regarded as an effective parameter (see Appendix A). Note that this expansion is only valid for displacements x which are small compared to the distance d between the SSET and the NR, i.e. $x \ll d$. Upon continuing the expansion, one encounters terms proportional to n^2 and to x^2 which will be neglected here.

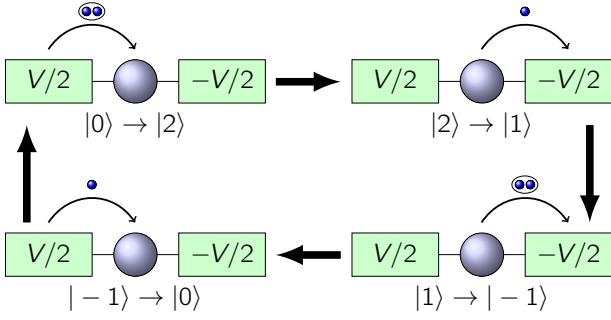


FIG. 2: Illustration of the DJQP cycle: (i) Cooper pair tunneling through the left junction, (ii) quasiparticle tunneling through the right junction, (iii) Cooper pair tunneling through the right junction and (iv) quasiparticle tunneling through the left junction.

Due to the complex structure of the full Hamiltonian (1) one should not hope for an exact solution in all regimes. Instead, we will make several assumptions which will enable us to investigate the transport properties of this system at a particular point in the parameter space.

First, we will briefly review the transport properties of the bare SSET without coupling to the NR. While the capacitances, Josephson energies and quasiparticle tunneling rates are essentially determined by the experimental setup, the most important tunable parameters are the bias voltage V and the gate voltage V_G . The transport properties of the SSET are then determined by how these voltages are related to the superconducting gap 2Δ and the charging energy E_C .

For high bias voltages $eV > 4\Delta$, the difference in chemical potentials allows quasiparticles on both junctions to overcome the superconducting gap and a quasiparticle current can flow. But even for lower bias voltages, one observes a finite current at certain values of the gate voltage. A possible mechanism is the Josephson-quasiparticle (JQP) resonance which is a cyclic process that starts with the tunneling of a Cooper pair on one of the junctions followed by two subsequent quasiparticle tunneling events on the other junction.^{38,42} This process is possible above a lower bias voltage threshold, $eV > 2\Delta + E_C$.

For even lower bias voltages, isolated current resonances can be observed which are due to the onset of the double Josephson quasiparticle (DJQP) resonance. A schematic picture of this process is shown in Fig. 2. It starts with a Cooper pair tunneling across, say, the left junction. Next, a quasiparticle tunnels out through the right junction, followed by a Cooper pair. Finally, after a quasiparticle tunnels through the left junction, the initial system state is reached again.

This process is energetically allowed only in a restricted parameter regime: Cooper pair tunneling is only possible if the chemical potentials of the lead and the island (taking into account the Coulomb energy) are on resonance while quasiparticle tunneling requires a difference

in chemical potentials sufficient to overcome the superconducting gap. For the DJQP process, it is easy to show that the resonances occur at bias voltages $eV = 2E_C$ and half-integer island charges n_0 .

The parameter regime which we investigate is therefore characterized by a charging energy E_C , a superconducting gap 2Δ and a bias voltage V which are of the same order of magnitude. Roughly speaking, these energy scales are very large compared to the quasiparticle tunneling rates $\Gamma_{L,R}$, the Josephson energies $J_{L,R}$ and the oscillator energy $\hbar\omega$.

A. Derivation of a Liouville equation

Due to the small tunneling rates, only sequential tunneling will contribute to the transport whereas higher-order (cotunneling) processes are suppressed. This suggests describing the system by a master equation in the Born-Markov approximation.

For this purpose, we treat the BCS Hamiltonians $H_L + H_R + H_I$ as a fermionic bath for the remaining system. Then, system and bath are only coupled by the quasiparticle Hamiltonian $H_{T,qp}$. Using the Born approximation corresponds to disregarding cotunneling processes while the Markov approximation is valid as long as there is a separation of time scales between the system and the bath degrees of freedom. Introducing the system and bath Hamiltonians

$$H_S = H_C + H_{T,CP} + H_N + H_{N,I}; \quad (8)$$

$$H_B = H_L + H_R + H_I; \quad (9)$$

and using the Born-Markov approximation leads to the following master equation for the reduced density matrix (t) of the system,

$$\begin{aligned} \dot{\rho}_S(t) &= L[\rho_S(t)] \\ &= \frac{i}{\hbar} [H_S; \rho_S(t)] \\ &\quad - \frac{1}{\hbar^2} \sum_{\alpha, \beta} \int_0^t d\tau \text{Tr}_B [H_{T,qp}; H_{T,qp}(\tau); \rho_S(t-\tau) \rho_B] \rho_S(t); \end{aligned} \quad (10)$$

where ρ_B is the bath density matrix. The time dependence of the $H_{T,qp}$ operator is governed by the Hamiltonian $H_S + H_B$. The density matrix contains information only about the charge and the oscillator degrees of freedom and can, for example, be written in the basis $|j; n_R; x_i\rangle$ of island charge states $|j\rangle$, the amount of charge j_R which has tunneled through the right junction, and the oscillator coordinate $|x_i\rangle$. This approach allows the calculation of the transport properties of the system via charge counting.^{43,44} In order to investigate the transport at the DJQP resonance, it is sufficient to consider a finite number of basis states for the island charge n . As a single DJQP cycle involves four charge states, we can restrict the basis to the states $|j-1\rangle$, $|j\rangle$, $|j+1\rangle$, and $|j+2\rangle$ which significantly reduces the complexity of

the problem, since it is thus sufficient to study a reduced density matrix as described in section II C. This choice of charge states corresponds to $n_0 = \pm 2$.

As long as one is only interested in oscillator properties or the current through the SSET, the j_R states can be traced out, and an effective master equation acting on the Hilbert space of island charge and oscillator position, spanned by the states $|j; x\rangle$, can be obtained. On the other hand, for the calculation of the current noise, the j_R degree of freedom has to be taken into account explicitly, as will be explained later on. For now, we proceed with the n_R -independent case.

As in the case of the JQP,⁴⁰ the Liouvillian obtained from Eq. (10) can be written as a sum of three contributions

$$L = L_{H_S} + L_{qp} + L_{CL}; \quad (11)$$

where L_{H_S} governs the coherent evolution of the system, L_{qp} is a dissipative term due to quasiparticle tunneling and L_{CL} is a Caldeira-Leggett type contribution introduced to model the coupling of the harmonic oscillator to a finite-temperature environment. Explicitly,

$$L_{H_S} = \frac{i}{\hbar} [H_S; \cdot]; \quad (12)$$

$$L_{qp} = L_{\hat{p}_{1;0}} \hat{p}_{1;0}^y - \frac{1}{2} L_{\hat{p}_{1;1}} \hat{p}_{1;1}^y g + L_{\hat{p}_{2;1}} \hat{p}_{2;1}^y - \frac{1}{2} L_{\hat{p}_{2;2}} \hat{p}_{2;2}^y g; \quad (13)$$

$$L_{CL} = \frac{D}{\hbar^2} [x; [x; \cdot]] - \frac{i \text{ext} M}{2\hbar} [x; f v; g]; \quad (14)$$

where $\hat{p}_{kj} = \langle j | i \hbar k \rangle$ acts on the charge states of the island and is utilized here to describe the quasiparticle tunneling event that changes the charge state from $|j\rangle$ to $|i\rangle$. The energy dependence of the quasiparticle tunneling rates L and R is weak and will therefore be neglected in the following. The diffusion constant D and external damping rate ext are related via a fluctuation-dissipation relation

$$\begin{aligned} D &= M \text{ext} \frac{\hbar}{2} \coth \frac{\hbar}{2k_B T_B} \\ &= M \text{ext} \sim \hbar n_{osc} i + \frac{1}{2} \end{aligned} \quad (15)$$

For $\hbar \ll k_B T_B$, the diffusion constant can be approximated by $D = M \text{ext} k_B T_B$.

In the general case, it is neither possible to calculate exactly the steady-state properties nor the transport properties of the coupled system using the Liouville superoperator (11). Thus, approximation schemes must be employed. In the following two subsections, we describe in detail the two complementary approximation schemes we use to study the coupled SSET-oscillator system.

B. Mean-field approach

Physical quantities can be calculated by evaluating the matrix elements of the density matrix $\rho(t)$. It turns out that oscillator properties and the average current can be written in terms of expectation values of the form

$$\langle x^n v^m \hat{p}_{kj} \rangle = \text{Tr}_{osc} \left(\sum_{n_R} \langle k; n_R | x^n v^m \rho(t) | j; n_R + k \rangle \right); \quad (16)$$

where x and v are the position and velocity operators of the oscillator and $\hat{p}_{kj} = \langle j | i \hbar k \rangle$. The trace over the oscillator degrees of freedom Tr_{osc} will be used in the position basis $\text{Tr}_{osc}(\cdot) = \int dx \langle x | \cdot | x \rangle$ as well as in the phonon number basis where $\text{Tr}_{osc}(\cdot) = \sum_{n_{osc}=0}^{\infty} \langle n_{osc} | \cdot | n_{osc} \rangle$. For the uncoupled SSET tuned closely to the DJQP resonance, the average current can be calculated straightforwardly, as taking the matrix elements of the master equation (10) leads to a closed set of equations.⁴³ If the NR is included, however, the coupling terms will lead to equations involving matrix elements of the form $\langle x \hat{p}_{kj} \rangle$. Calculating their time evolution leads to ever higher-order terms of the form $\langle x^n v^m \hat{p}_{kj} \rangle$, so that the set of differential equations never closes. Hence, a truncation scheme is needed. A standard route is to truncate the system of equations by assuming a vanishing n th-order cumulant $\langle x^n \hat{p}_{kj} \rangle$. This allows one to rewrite n th-order expectation values in terms of expectation values of order $n-1$ and hence to arrive at a closed, albeit non-linear, set of equations.

We use and compare these approximations for $n=1$ (which we call the *mean-oscillator approximation*) and $n=2$ (Gaussian approximation). These two levels of approximation are related to what was called *mean 1'* and *mean 2'* in Ref. [40]. In order to give an estimate of the physical quality of the truncation scheme, we also compare our results to exact numerical calculations.

Whereas the expectation values of the form (16) are sufficient for the calculation of the oscillator properties and the SSET current, the calculation of the noise requires a slightly extended approach. In order to keep track of the transferred charge, one has to investigate the dynamics of n_R -resolved expectation values. It turns out (see Appendix E) that the noise can be rewritten in terms of expectation values of the operators

$$\hat{p}_{kj}^{n_R 0} = \langle j | i \hbar n_R \rangle; \quad (17)$$

Note that only elements which conserve the number of charges, $j + n_R = k + n_R^0$, are finite. An analogous truncation scheme can be applied to expectation values containing these operators. Similar approaches have been used extensively to describe nanoelectromechanical systems.^{8,40,44,45,46,47,48}

C. Numerical solution of the Liouville equation

To complement the analytical mean-field approach described in the last subsection, we also use a numerical

approach to study the properties of the NR coupled to an SSET near the DJQP resonance. First, we present the approach taken for the calculation of the current and the oscillator properties, where the n_R degree of freedom plays no role. Subsequently, we will demonstrate how to extend this approach for the noise calculation, where n_R has to be taken into account.

To calculate the current and the oscillator properties, we write the density matrix in the $|j; n_{\text{osc}}\rangle$ basis, with n_{osc} being the phonon quantum number of the oscillator and n the charge of the SSET. The spectrum of the harmonic oscillator is naturally not finite, so we need to truncate it and consider only its N_{max} lowest energy eigenstates. To describe the DJQP cycle, the reduced density matrix is of dimension $(4N_{\text{max}} \times 4N_{\text{max}})$.

The Liouville superoperator L is a two-sided operator, in the sense that it acts both from the left and the right of the density matrix [cf. Eq. (12)]. It can be transformed to a single-sided operator using a property of the matrix vectorization operation: the vectorized form of a product of three $(4N_{\text{max}} \times 4N_{\text{max}})$ matrices A, B, C can be written as a single product of an $(16N_{\text{max}}^2 \times 16N_{\text{max}}^2)$ matrix with an $(16N_{\text{max}}^2 \times 1)$ vector via the relation $\text{vec}(ABC) = (C^T \otimes A) \text{vec}(B)$, where the superscript T denotes the matrix transposition and \otimes a Kronecker product.⁶⁹ The matrix representation of the Liouville superoperator is therefore of order $(16N_{\text{max}}^2 \times 16N_{\text{max}}^2)$.

To illustrate how the aforementioned vector identity can be used, we apply it to the coherent evolution contribution to the Liouville equation [Eq. (12)]. In this case, we find

$$\begin{aligned} L_{H_S} &= \frac{i}{\hbar} [H_S; \cdot]; \\ \text{vec}(L_{H_S}) &= \frac{i}{\hbar} \mathbf{I} \otimes H_S + H_S^T \otimes \mathbf{I} \text{vec}(\cdot); \end{aligned} \quad (18)$$

where the matrix representation of the identity matrix \mathbf{I} and of the system Hamiltonian H_S is of order $(4N_{\text{max}} \times 4N_{\text{max}})$.

To find the vectorized form of the stationary density matrix ρ_{stat} , defined from $L \rho_{\text{stat}} = 0$, we calculate the null-space of the Liouville matrix. Using the normalization condition $\text{Tr}[\rho_{\text{stat}}] = 1$, the stationary density matrix ρ_{stat} can be determined uniquely. The bad scaling $O(N_{\text{max}}^4)$ of the Liouvillian size with the truncation point in the oscillator spectrum makes the numerical eigenvalue problem very challenging. Luckily, in this problem the Liouville matrix displays a high sparsity degree, and sparse eigensolvers can be used. Our implementation uses the shift-invert mode of the ARPACK⁴⁹ eigensolver in combination with the PARDISO^{50,51} linear solver to compute the first few (~ 5) eigenvalues of L with the lowest magnitude (~ 0) as well as the associated eigenvectors. The calculated magnitude of the smallest eigenvalue can be used to verify the validity of the truncation scheme: when enough Fock states are kept we find $j_0 j < 10^{-15}$ which is below the desired precision limit of 10^{-10} .

To improve the speed of the calculation and, more

importantly, to increase numerical accuracy, we do not need to explicitly solve for those matrix elements of ρ_{stat} which, due to the considered Hamiltonian, have to be zero. For example, coherence can only be created between two charge states $|k\rangle$ and $|j\rangle$ if $|k - j| = 2$, since only these pairs of states are coupled by Josephson tunneling. Therefore, all density-matrix elements ρ_{kj} where $|k - j|$ is odd are zero. Using this argument, the size of the Liouville matrix can be reduced to $(8N_{\text{max}}^2 \times 8N_{\text{max}}^2)$.

The use of sparse solvers also minimizes the required memory for the calculation of the eigenvalues, allowing problems of relatively large size ($N_{\text{max}} \sim 150$) to be solved on a desktop computer. Also, we note that, contrary to what was discussed in Ref. [52], no manual preconditioning was needed to achieve high numerical accuracy. To allow for the numerical approach to be used in the driving regime, where we expect the average energy of the oscillator to be relatively high, we had to make a supplementary approximation. In this case, we assumed that coherence could develop only between states of the oscillator that are not too far away in energy from each other, setting $\langle n_{\text{osc}} | j \rangle \langle n_{\text{osc}} | i \rangle = 0$ for $|n_{\text{osc}} - n_{\text{osc}}'| > 60$. This allowed for N_{max} to be set as high as 750 on a standard workstation. Moreover, in the cases where it was possible to compare directly the results of the calculation with and without this last approximation, we found that they were identical (within our numerical accuracy).

While this approach is viable for the calculation of the oscillator properties and the current, it fails to keep track of the tunneled charge n_R and thus cannot be used to calculate the current noise. A straightforward inclusion of the $|j, n_R\rangle$ states is numerically impossible as the corresponding Hilbert space is of infinite dimension. However, this problem can be circumvented by considering the n_R -resolved density matrices $\rho_{(n_R)}^{(n_R)}$ ($n_R \in \mathbb{Z}$), which are submatrices of the complete density matrix ρ , whose entries are defined by

$$\rho_{kj}^{(n_R)} = \langle k; n_R | \rho | j; n_R \rangle; \quad (19)$$

where the relation between n_R and n_R^0 is given by charge conservation. At the DJQP resonance, we have $n_R^0 = n_R - 2$ for $(k; j) = (1; 1)$, $n_R^0 = n_R + 2$ for $(k; j) = (-1; 1)$ are $n_R^0 = n_R$ otherwise.⁴³ Note that we did not write out the oscillator degree of freedom explicitly in this matrix. Calculating the time evolution of these matrix elements according to Eq. (10), one finds

$$\begin{aligned} \frac{d}{dt} \rho_{(n_R)}^{(n_R)} &= L \rho_{(n_R)}^{(n_R)} + I_{\text{qp}}^+ \rho_{(n_R-1)}^{(n_R-1)} + I_{\text{qp}}^- \rho_{(n_R+2)}^{(n_R+2)} + I_{\text{CP}} \rho_{(n_R-2)}^{(n_R-2)}; \end{aligned} \quad (20)$$

As expected, the tunneling leads to a coupling between density matrices of different n_R . It is produced by the current superoperators describing the quasiparticle and

the Cooper pair tunneling, which are defined as

$$\begin{aligned} I_{qp} &= \text{Tr} [j_{lh} j_{rh} j_{rh} j_{lh}]; \\ I_{CP}^+ &= \frac{iJ_R}{2\omega} [j_{lh} j_{rh} j_{rh} j_{lh} + j_{lh} j_{rh} j_{lh} j_{rh}]; \\ I_{CP} &= \frac{iJ_R}{2\omega} [j_{lh} j_{rh} j_{rh} j_{lh} + j_{lh} j_{rh} j_{lh} j_{rh}]; \end{aligned} \quad (21)$$

It is important to realize that by writing the Liouville equation in terms of n_R -resolved density matrices and current superoperators, we have achieved a description of the system in terms of only the $|j; n_{osc}\rangle$ states again. This, however, comes at the price of having to deal with an infinite number of density matrices, (n_R) . Still, following the approach of Ref. [53] it will turn out that convenient expressions for the current and the noise can be formulated in terms of these current superoperators.

III. OSCILLATOR PROPERTIES

As mentioned before we treat the NR as a harmonic oscillator and we use the master equation to investigate the time evolution of the mean displacement

$$\langle x \rangle = \text{Tr}_{n_R} \text{Tr}_n \text{Tr}_{osc} [\rho(t) x]; \quad (22)$$

and of the velocity v , correspondingly. Here, $\text{Tr}_n(\cdot) = \sum_{n=-1}^2 \text{Tr}_j \cdot$ denotes the trace over the island charge, while $\text{Tr}_{n_R}(\cdot) = \sum_{n_R=-1}^1 \text{Tr}_j \cdot$ traces over the tunneled charge. Likewise, the master equation will allow us to calculate expectation values of higher order like $\langle x^2 \rangle$ and $\langle v^2 \rangle$ which are required for the calculation of the oscillator energy.

For a linear coupling of the NR to the SSET as in Eq. (7), we find the following equations describing the time evolution of the oscillator coupled to the SSET

$$\frac{d}{dt} \langle x \rangle = \langle v \rangle; \quad (23)$$

$$\frac{d}{dt} \langle v \rangle = -\omega^2 \langle x \rangle - \gamma_{ext} \langle v \rangle + \frac{A}{M} \langle n \rangle; \quad (24)$$

where $\langle n \rangle = \sum_k P_k \langle n_k \rangle$ is the expectation value of the island occupation and γ_{ext} accounts for the external damping. The stationary limit, where $\frac{d}{dt} \langle v \rangle = \frac{d}{dt} \langle x \rangle = 0$, can be regarded as the long-time limit when the oscillatory behavior has been damped by the thermal bath and thus $\langle v \rangle = 0$ and $\langle x \rangle = (A/M\omega^2) \langle n \rangle$. If the coupling A to the SSET is zero, the oscillator stays in its equilibrium position at $\langle x \rangle = 0$. For finite coupling, due to the electromagnetic repulsion the NR equilibrates in a position $\langle x \rangle \neq 0$ proportional to the coupling and the charge $\langle n \rangle$ on the island. Note that the influence of the SSET on the NR is of the first order in the coupling A . This regime has already been studied in some detail^{8,9} and it was shown that the SSET acts as an effective thermal bath for the NR. As we will illustrate further on, the signature of the NR in the transport properties of the SSET is of second

order in the coupling and is clearly visible in the current and the noise properties of the SSET.

To study the influence of the NR on the SSET we introduce dimensionless quantities which are normalized to motional quanta of the oscillator. Using the frequency and the harmonic oscillator length,

$$x_0 = \sqrt{\frac{\hbar}{2M\omega}}; \quad (25)$$

as units we define $\tilde{x} = x/x_0$, $\tilde{t} = \omega t$ and $\tilde{v} = v/x_0$, i.e. we normalize all variables with respect to "oscillator" quantities. This allows an easier comparison with the experiment where, for example, the bias voltage can be varied at constant coupling. Consequently, the equations of motion can be rewritten as

$$\frac{d}{d\tilde{t}} \langle \tilde{x} \rangle = \langle \tilde{v} \rangle; \quad (26)$$

$$\frac{d}{d\tilde{t}} \langle \tilde{v} \rangle = -\langle \tilde{x} \rangle - \tilde{\gamma}_{ext} \langle \tilde{v} \rangle + 2\tilde{A} \langle \tilde{n} \rangle; \quad (27)$$

where $\tilde{\gamma}_{ext} = \gamma_{ext}/\omega$ and $\tilde{A} = x_0 A/\hbar\omega$.

Not only is the equilibrium position of the resonator shifted by the coupling to the SSET, but also the cumulants of the position and velocity of the NR, i.e. $\langle \tilde{x}^2 \rangle = \langle x^2 \rangle/x_0^2$, $\langle \tilde{x} \tilde{v} \rangle$, are influenced by this coupling:

$$\frac{d}{d\tilde{t}} \langle \tilde{x}^2 \rangle = \langle \tilde{x} \tilde{v} + \tilde{v} \tilde{x} \rangle; \quad (28)$$

$$\begin{aligned} \frac{d}{d\tilde{t}} \langle \tilde{x} \tilde{v} + \tilde{v} \tilde{x} \rangle &= 2\langle \tilde{v}^2 \rangle - 2\langle \tilde{x}^2 \rangle - \tilde{\gamma}_{ext} \langle \tilde{x} \tilde{v} + \tilde{v} \tilde{x} \rangle \\ &+ 4\tilde{A} (\langle \tilde{n} \tilde{x} \rangle - \langle \tilde{n} \tilde{v} \rangle); \end{aligned} \quad (29)$$

$$\begin{aligned} \frac{d}{d\tilde{t}} \langle \tilde{v}^2 \rangle &= \langle \tilde{x} \tilde{v} + \tilde{v} \tilde{x} \rangle - 2\tilde{\gamma}_{ext} \langle \tilde{v}^2 \rangle + 4\tilde{\gamma}_{ext} \tilde{T}_B \\ &+ 4\tilde{A} (\langle \tilde{n} \tilde{v} \rangle - \langle \tilde{n} \tilde{x} \rangle); \end{aligned} \quad (30)$$

where $\tilde{T}_B = k_B T_B/\hbar\omega$ and f_{\pm} denotes the anti-commutator. In the stationary limit this leads to

$$\langle \tilde{x} \tilde{v} + \tilde{v} \tilde{x} \rangle = 0; \quad (31)$$

$$\langle \tilde{v}^2 \rangle = 2\tilde{T}_B + 2\tilde{A} (\langle \tilde{n} \tilde{v} \rangle - \langle \tilde{n} \tilde{x} \rangle) = \tilde{\gamma}_{ext}; \quad (32)$$

$$\langle \tilde{x}^2 \rangle = \langle \tilde{v}^2 \rangle + 2\tilde{A} (\langle \tilde{n} \tilde{x} \rangle - \langle \tilde{n} \tilde{v} \rangle); \quad (33)$$

To lowest (linear) order, which we refer to as the thermal-oscillator approximation, we assume that $\langle \tilde{n} \tilde{v} \rangle = \langle \tilde{n} \tilde{x} \rangle$. This is identical to assuming that the correlations between n and v vanish, i.e. $\langle \tilde{n} \tilde{v} \rangle = 0$. Consequently, the fluctuations of the harmonic oscillator are not influenced by the SSET such that the virial theorem $\langle \tilde{v}^2 \rangle = \langle \tilde{x}^2 \rangle$ and the equipartition theorem $\langle \tilde{v}^2 \rangle = 2\tilde{T}_B$ are fulfilled in the high-temperature limit $\tilde{T}_B \gg 1$. The resonator is thus in a thermal state determined only by \tilde{T}_B and $\tilde{\gamma}_{ext}$. In the thermal-oscillator approximation analytic expressions for the current and noise in the SSET can be derived and will be discussed in the upcoming sections.

The thermal-oscillator approximation is justified for weak coupling between the SSET and the NR, but fails for stronger coupling, since the observables of the oscillator become entangled with the charge state of the SSET. As was already observed before,^{8,9} an increased coupling can drive the oscillator to a non-thermal state characterized by a finite $\langle \dot{x} \rangle \neq 0$, where the virial and equipartition theorems no longer hold.

In order to investigate this regime, we have to go to the next order in our approximation which means taking the fluctuations of \dot{x} into account, but assuming all higher-order cumulants to vanish, e.g. $\langle \dot{x}^2 \rangle = 0$. This will be referred to as the Gaussian approximation since for a Gaussian distribution all cumulants $\langle \dot{x}^n \rangle$ for $n > 2$ are zero and the resonator is fully described by the two lowest moments. Under this assumption, we can express expectation values of the form $\langle \dot{x}^2 \rangle$ as products of the lower-order expectation values $\langle \dot{x} \rangle$, $\langle \dot{x}^2 \rangle$, $\langle \dot{x} \rangle$ and $\langle \dot{x} \rangle$. While this approach leads to a closed set of differential equations, the set will now be non-linear and has to be solved numerically.

In principle, this approximation scheme can be continued to even higher orders.⁴⁰ However, since the Gaussian approximation works well for the low-coupling regime we are interested in, we do not go beyond it. Ultimately, for even stronger coupling, the linear coupling between the SSET and the NR itself becomes questionable.

In order to investigate the oscillator state in more detail, we study the energy $E = \frac{1}{2}M \dot{x}^2 + \frac{1}{2}M \omega^2 x^2$, in dimensionless quantities

$$\frac{E}{\hbar\omega} = \frac{1}{4} \dot{x}^2 + \frac{1}{2} x^2 = \langle \dot{x}^2 \rangle + \frac{1}{2} : \quad (34)$$

Previous work^{9,46} has focused on the fluctuations of the number of charges on the island, n , which in linear response can be described by an effective damping and effective temperature. We will discuss this approach in more detail in the context of the charge noise. For an identification of the oscillator state, though, we choose a different route and investigate the energy of the NR. In the stationary limit, using Eqs. (32) and (33), we find for the energy

$$\frac{E}{\hbar\omega} = T_B + \tilde{A} \frac{2\langle \dot{x} \rangle + \tilde{\omega}_{\text{ext}} \langle \dot{x} \rangle}{2\tilde{\omega}_{\text{ext}}} + \frac{1}{4} \langle \dot{x} \rangle^2 : \quad (35)$$

A finite $\langle \dot{x} \rangle \neq 0$ provides additional potential energy, but the contribution is small, since $\langle \dot{x} \rangle^2 = 4\tilde{A}^2 \langle \dot{x} \rangle^2$. Therefore, it is the correlations of the entangled SSET-NR system contained in the second term, which have the potential to drive the system out of a thermal state.

The results for a calculation of the energy in the Gaussian approximation for a typical, experimentally relevant set of parameters are shown in Figs. 3 and 4 where we display the oscillator energy as a function of gate voltage V_G and the bias voltage V measured away from the resonance position. As the DJQP cycle contains two Cooper pair tunneling events, there are two resonance conditions

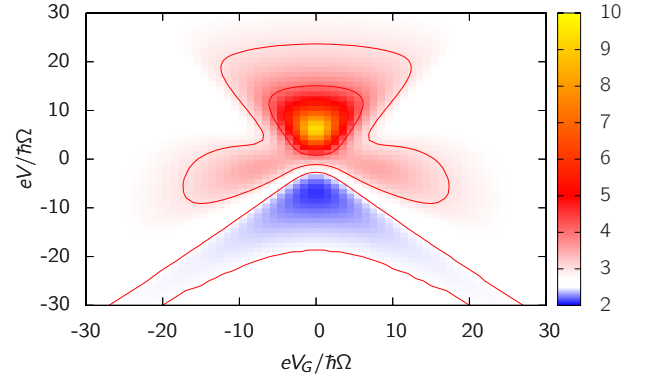


FIG. 3: Oscillator energy in units of $\hbar\omega$ in the Gaussian approximation as a function of the gate voltage $eV_G = \hbar\Omega$ and the bias voltage $eV = \hbar\omega$ where $(0;0)$ denotes the resonance. The parameters used are $\tilde{\omega}_L = \tilde{\omega}_R = 10$; $\tilde{J}_L = \tilde{J}_R = 2$; $\tilde{\omega}_{\text{ext}} = 10^{-4}$, $T_B = 2.5$ and $\tilde{A} = 0.02$. In the red-detuned area ($V < 0$, $V < V_G < V$), cooling below the bath temperature is visible (blue region). Driving can be observed in the blue-detuned case ($V > 0$, $V < V_G < V$). The highest energies are obtained in the yellow region.

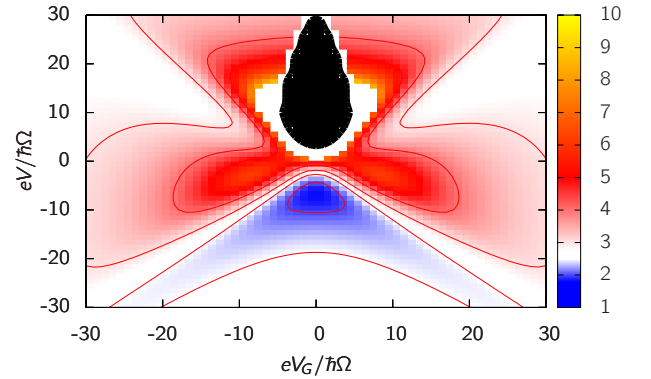


FIG. 4: Oscillator energy in the Gaussian approximation in units of $\hbar\omega$ for the Gaussian approximation as a function of the gate voltage $eV_G = \hbar\Omega$ and the bias voltage $eV = \hbar\omega$ for increased coupling $\tilde{A} = 0.03$. Cooling and driving effects are increased as compared to Fig. 3. In the black area two stable and one unstable solution are found, i.e. the system becomes bistable. The area grows for stronger coupling.

which have to be met and which can be controlled by adjusting the bias and gate voltages.

The physical picture can be explained most clearly if we assume $V_G = 0$, which corresponds to a vertical cut in Fig. 3. If the system is blue-detuned from a resonance ($V > 0$), the tunneling Cooper pairs transfer a part of their energy to the oscillator in order to be able to tunnel. This leads to driving of the oscillator. On the contrary, for a red-detuned resonance ($V < 0$), the Cooper pairs can absorb energy from the oscillator, leading to cooling. A similar result was already found using a linear-response approach in Ref. [9].

In the regime where both resonances involved in the DJQP cycle are blue-detuned ($V > 0$, $V < V_G < V$),

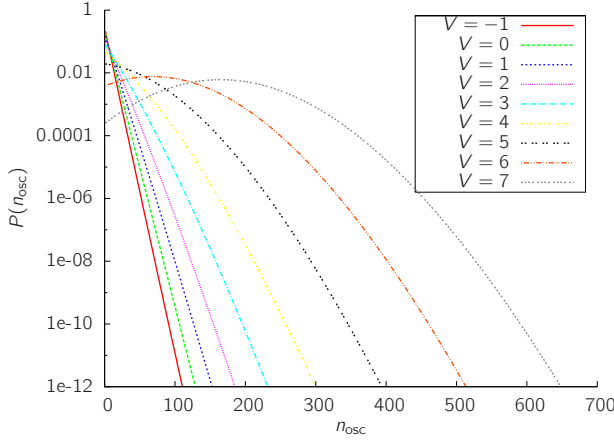


FIG. 5: Distribution $P(n_{\text{osc}})$ of the oscillator phonon number for different values of the bias voltage $eV = \sim = f \cdot 1; 0; 1; \dots; 7\gamma$ from left to right along the x-axis. The parameters used for this plot are $\tilde{A} = 0.1$, $\tilde{\omega}_L = \tilde{\omega}_R = 12$, $\tilde{J}_L = \tilde{J}_R = 2.5$, $\tilde{\omega}_{\text{ext}} = 0.001$ and $T_B = 3$. For negative V and small positive V we find an exponential decay corresponding to a thermal state. For larger $V > 0$ the distribution develops a peak at $n \neq 0$ which indicates a driven state.

we find a particularly strong driving of the oscillator. In the white regions of Fig. 4, energies of the order $10^3 \sim$ (depending on the system parameters) are reached even for rather small coupling of the order $\tilde{A} \sim 0.02$. The numerical solution of the Liouville equation reveals moreover that the resulting oscillator state is highly non-thermal, i.e. the distribution function of oscillator states $P(n_{\text{osc}})$ strongly deviates from a Boltzmann distribution.

This is calculated in Fig. 5 using the numerical approach for different values of $eV = \sim$. We find an exponential decay for $V \leq 0$ corresponding to the high-temperature limit of the Boltzmann distribution and a trend towards a driven state for $V > 0$.

In the regime where both resonances are red-detuned ($V < 0$, $V < V_G < V$), we find a cooling of the oscillator to temperatures well below the bath temperature. This shows up in Figs. 3 and 4 as the little triangular-shaped regions below the center, where the oscillator energy drops below the value corresponding to the bath temperature.

Due to the non-linearity of the master equation, more than one physical solution may emerge and we find that this is indeed the case in the sector where the NR is strongly driven. An analogous effect was found previously for the same system at the JQP cycle⁴⁰ and for a more general class of systems.^{53,54,55,56,57,58} We find that generally, the response of the system close to a DJQP resonance is much more pronounced than at the JQP in the sense that quantitatively similar effects may be observed at much smaller values of the coupling. This agrees with the prediction⁹ that the backaction effects at the DJQP exceed those of the JQP by a factor $(\omega = J)^4$. Therefore the DJQP is favorable from the experimental point of

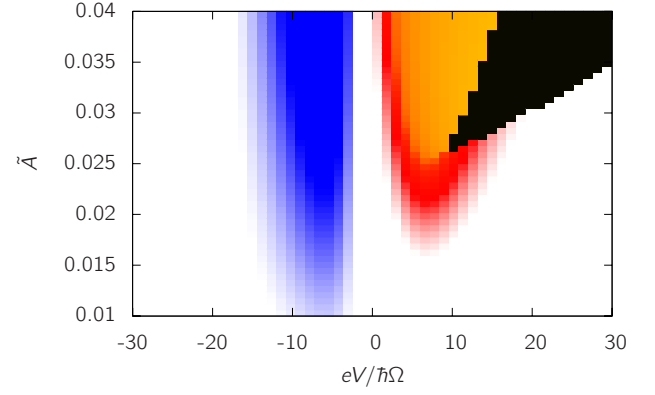


FIG. 6: Oscillator energy in arbitrary units as a function of bias voltage $eV = \sim$ and coupling \tilde{A} calculated in the Gaussian approximation. For $V < 0$, backaction leads to cooling of the oscillator (blue). On the contrary, strong driving (red/yellow) can be observed for $V > 0$. Above a critical coupling $\tilde{A}(V)$, the system enters a bistable region (black). The parameters are the same as in Fig. 3 and $eV_G = \sim = 0$.

view since achieving a strong coupling is challenging.

A plot of the location of the bistabilities found in the Gaussian approximation as a function of the bias voltage V and the coupling strength \tilde{A} is shown in Fig. 6. A gain, cooling of the oscillator is seen in the blue regions for $V < 0$, whereas driving happens for $V > 0$ as is depicted by red regions. Towards stronger coupling, both effects increase in magnitude. Two stable solutions appear only for a blue-detuned SSET and the voltage range where such an effect is visible grows with increased coupling. When increasing the coupling for a given voltage $V > 0$ (which corresponds to a vertical cut in Fig. 6), the system will evolve from a thermal state via the bistable state to a single driven state. On the contrary, an increase in voltage (corresponding to a horizontal cut) carries the system from a thermal state to a driven state, then into the bistable region. Beyond the bistable region, the system will fall back to the thermal state. Note that the effect of driving is much stronger than the cooling of the NR (cf. Figs. 3 and 4).

We have confirmed the existence of bistability using the numerical approach by explicitly calculating the complete probability distribution $P(x)$ [results not shown explicitly]. In a thermal state, this distribution shows a single peak at $x = 0$. In a driven state, on the contrary, two symmetric peaks at finite values $|x| \neq 0$ appear. In the bistable regime, the system switches between these two states, leading to a distribution $P(x)$ that shows three peaks, one (thermal) at the origin and two side-peaks (driven) at $|x| > 0$. From these studies of the bistable regime using the numerical approach, we noticed that the parameter range in which the system exhibits bistability is smaller than the one obtained via the mean-field solution. The structure of the bistable region could be better predicted using the analytical approach by including higher than second order cumulants, i.e. extending

the analysis beyond the Gaussian approximation.

In the following sections, we will show that these different states of the NR also manifest themselves in the transport properties of the SSET, i.e. the current and the current noise.

IV. CURRENT PROPERTIES

We showed in the previous section that the coupling of an SSET to an NR can drive the oscillator into a non-thermal state and effect in cooling, potentially even cooling down close to the ground state.^{9,10} In the following, we will study if and how it is possible to measure signatures of the resonator state in the current and current noise characteristics of the SSET close to the DJQP resonance.

The number of electrons that have left the island to the right lead, n_R , is proportional to the transported charge and therefore determines the current flow. Hence, the expectation value of the current is given by

$$\langle I \rangle = \langle e \rangle \frac{d}{dt} \langle n_R \rangle = \langle e \rangle \text{Tr} \{ \dot{\rho}(t) \hat{n}_R \} \quad (36)$$

Without loss of generality, we chose to measure the current across the right junction. In the stationary limit, the total current is conserved such that the currents across the left and right junctions are equal. In each DJQP cycle, two tunneling events take place at the right junction, see Fig. 2: the transfer of a quasiparticle which takes the island from charge state $|i\rangle$ to the state $|j\rangle$. Subsequently, a Cooper pair tunnels to the right lead and leaves the island in the state $|j-1\rangle$. Two processes involving only changes in n_L and n , which therefore do not contribute to $\langle I \rangle$, close the cycle in which 3 electrons in total have been transported through the island.

Equivalently, in the stationary state the expectation value of the current $\langle I \rangle$ can be written using the superoperator formalism. From Eq. (20), one finds

$$\langle I \rangle = \langle e \rangle \text{Tr} \{ \hat{T}_R \text{Tr}_{\text{osc}} (I_{\text{total}}^{\text{stat}}) \} \quad (37)$$

where $I_{\text{total}} = I_{\text{qp}} - 2I_{\text{CP}}^+ + 2I_{\text{CP}}^-$ is the superoperator describing the total current. Equation (37) is used in this form in the numerical routine.

For the analytic mean-field approximation we split the total current into two terms, $\langle I \rangle = \langle I^{\text{ND}} \rangle + \langle I^{\text{D}} \rangle$, corresponding to a contribution from the tunneled Cooper pair (the non-dissipative current) I^{ND} , and a contribution from the quasiparticle tunneling event (the dissipative part) I^{D} . For these two contributions we can write down the exact expressions for the dissipative

$$I^{\text{D}} = \langle e \rangle \text{Tr} \{ \hat{T}_R \text{Tr}_{\text{osc}} (I_{\text{qp}}^{\text{stat}}) \} \quad (38a)$$

$$= \langle e \rangle_R \langle \hat{n}_{22} \rangle \quad (38b)$$

and non-dissipative part

$$I^{\text{ND}} = \langle e \rangle \text{Tr} \{ \hat{T}_R \text{Tr}_{\text{osc}} [2I_{\text{CP}}^+ - 2I_{\text{CP}}^-]_{\text{stat}} \} \quad (39a)$$

$$= \langle e \rangle 2i \langle \hat{n}_{1,-1} \rangle - \langle \hat{n}_{0,1} \rangle \quad (39b)$$

In the thermal-oscillator approximation, these expectation values can be calculated by solving for the corresponding elements of the density matrix, as shown in detail in the Appendix B. We find that the vector of all finite $\langle \hat{n}_{ji} \rangle$, \mathbf{j} , is given by $\mathbf{j} = i\mathbf{J}_L \mathbf{M}^{-1} \mathbf{j}$ where \mathbf{M} is the evolution matrix of the SSET system containing all the system parameters, Eq. (B3), and the constant \mathbf{j} is the inhomogeneous part of the master equation due to the normalization of the density matrix $\sum_k \langle \hat{n}_{kk} \rangle = 1$. Using this result the stationary current for the DJQP cycle can be written as

$$\langle I \rangle = \frac{3}{2} \langle e \rangle \left(\frac{1}{\tilde{\gamma}_R} + \frac{1}{\tilde{\gamma}_L} + \frac{1}{\tilde{\gamma}_L(\mathbf{x})} + \frac{1}{\tilde{\gamma}_R(\mathbf{x})} \right)^{-1} \quad (40)$$

The inverse of the tunneling rates for quasiparticles and Cooper pairs, $\tilde{\gamma}_{L,R}$ and $\tilde{\gamma}_{L,R}$, respectively, can be interpreted as effective resistances for these processes. Then, Eq. (40) is reminiscent of the current through a series of resistors, where the largest resistance determines the behavior. The Cooper pair tunneling rates are given by³⁸

$$\tilde{\gamma}_L(\mathbf{x}) = 2\tilde{\gamma}_R \frac{J_L^2}{(\tilde{\gamma}_R = 2)^2 + \frac{J_L^2}{2}(\mathbf{x})} \quad (41)$$

$$\tilde{\gamma}_R(\mathbf{x}) = 2\tilde{\gamma}_L \frac{J_R^2}{(\tilde{\gamma}_L = 2)^2 + \frac{J_R^2}{2}(\mathbf{x})} \quad (42)$$

where ϵ_{jk} denotes the difference in energy between the charge states $|j\rangle$ and $|k\rangle$ and thus measures the detuning from the DJQP resonance. The renormalized tunneling rates of the SSET are defined by $\tilde{\gamma} = \gamma / J$ and $\tilde{J} = J / 2\tilde{\gamma}$. If the Cooper pair tunneling, say, to the right lead is resonant, i.e. $\epsilon_{1,-1} = 0$, the rate $\tilde{\gamma}_R$ reaches a maximum at the value $\tilde{\gamma}_R = 8J_R^2 = \tilde{\gamma}_L = (2J_R^2 = \tilde{\gamma}_L) = \dots$. It decays like a Lorentzian away from the resonance. Expressions for the current in less general form are for example derived for $\epsilon_{jk} = 0$ in Ref. [43] and for $\epsilon_{1,-1} = \epsilon_{2,0}$ in Ref. [59].

Due to the capacitive coupling of the SSET to the NR, the resonance is shifted compared to the uncoupled case in the thermal approximation. We find in dimensionless units (derivation given in Appendix B)

$$\epsilon_{1,-1}(\mathbf{x}) = \frac{eV_G}{\tilde{\gamma}} + \frac{eV}{\tilde{\gamma}} - 2\tilde{A}\tilde{h}\mathbf{x} \quad (43)$$

$$\epsilon_{2,0}(\mathbf{x}) = \frac{eV_G}{\tilde{\gamma}} - \frac{eV}{\tilde{\gamma}} - 2\tilde{A}\tilde{h}\mathbf{x} \quad (44)$$

where $eV = \tilde{\gamma}$ and $eV_G = \tilde{\gamma}$ are the relative bias and gate voltages measured from the values at the DJQP resonance.

The SSET is affected only if the average position of the NR is finite, i.e. $\tilde{h}\mathbf{x} \neq 0$. This shift in the equilibrium position of the NR effectively corresponds, from the point of view of the SSET, to a change in V_G and will therefore be referred to as an effective backgate behavior later on. This effect is of second order in the coupling A since we observed in the previous section that $\tilde{h}\mathbf{x}$ is linear in A .

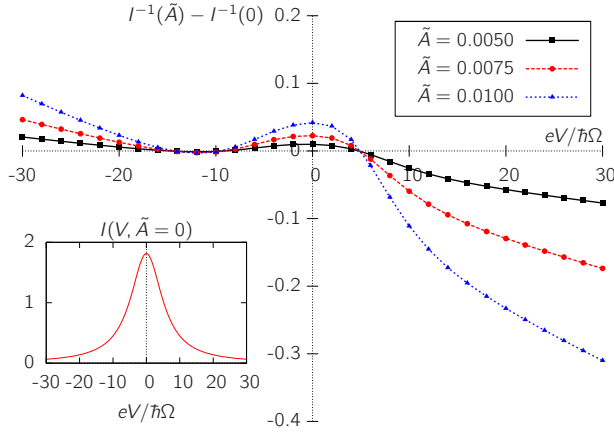


FIG. 7: Difference of the inverse current $I^{-1}(\tilde{A}) - I^{-1}(\tilde{A} = 0)$ versus bias voltage $eV/\hbar\Omega$ for various coupling strengths \tilde{A} . From the intersection with the voltage axis, the shift $2\tilde{A}\hbar\omega$ of the oscillator position can be read out. Lines correspond to the numerical analysis and agree well with the Gaussian approximation (points) in this parameter regime. Inset: Average current $\hbar I$ through the SSET for the parameters $\tilde{\gamma}_L = \tilde{\gamma}_R = 10$, $J_L = J_R = 2$, $\tilde{\gamma}_{\text{ext}} = 10^{-4}$, and $T_B = 3$.

Note that the average displacement of the NR oscillation in the stationary limit,

$$\hbar\bar{x} = 2\tilde{A}\hbar\bar{n} = 2\tilde{A} \left(\frac{1}{\tilde{\gamma}_R} + \frac{1}{R(\tilde{x})} \right) \frac{2\hbar I}{3(e)}; \quad (45)$$

is determined by the Cooper pair tunneling rate R in addition to the quasiparticle tunneling rate $\tilde{\gamma}_R$. This is in contrast to the JQP cycle where it is only the necessarily small $1/\tilde{\gamma}_R$ which determines the displacement. Since the rates and the current are implicitly dependent on $\hbar\bar{x}$ via the Cooper pair tunneling rate, Eq. (45) is a self-consistency equation.

Going beyond the thermal-oscillator approximation, we use again the truncated master equation and the numerical approach to calculate the current via the general Eqs. (38) and (39). In order to assess the quality of the Gaussian approximation, we first compare the results of the two approaches for low coupling strength. The result is shown in Fig. 7, where we plot the difference in the inverse current between the weakly coupled and the uncoupled system. The results of the Gaussian approximation and the numerically evaluated lines are in excellent agreement. The Lorentzian lineshape of the current (inset of Fig. 7) is preserved in case of the weak coupling.

The change in the average current due to the coupling to the oscillator can be most transparently illustrated by plotting the difference of the inverse currents in the coupled and the uncoupled cases, see Fig. 7. As obvious from Eq. (40) the inverse current $I^{-1}(\tilde{A})$ is given by the sum of rates involving the various transport processes. In the thermal-oscillator approximation, the function $I^{-1}(\tilde{A}) - I^{-1}(\tilde{A} = 0)$ changes sign as a function of $eV/\hbar\Omega$ at a position which is proportional to $2\tilde{A}\hbar\bar{x}$ as

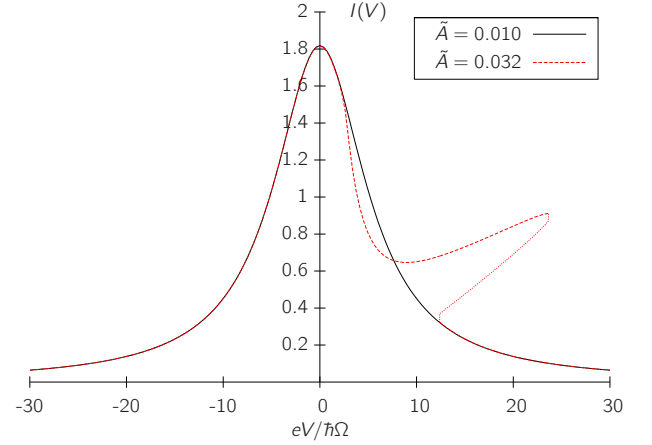


FIG. 8: Average current $\hbar I$ versus bias voltage for $\tilde{A} = 0.01$ and $\tilde{A} = 0.032$, $T_B = 2.5$, further parameters as in Fig. 7. For increased coupling the Lorentzian peak becomes distorted and two stable solutions emerge which result in two stable values for the current.

is shown in Eq. (B15). We expect this sign change to be the most feasible way to experimentally observe the influence of the NR on the SSET current and to investigate quantitatively the coupling strength using only the average current.

The bistability of the oscillator states, which was already discussed in the previous section, also manifests itself in the current through the SSET. For increased coupling, we find that the equation of motion derived within the Gaussian approximation has up to three solutions, of which two correspond to stable currents. The resulting current-voltage characteristic is shown in Fig. 8. In the center, the usual JQP resonance is clearly visible. While for very low coupling $\tilde{A} = 0.01$, the current still follows approximately a Lorentzian, strong deviations become visible already for $\tilde{A} = 0.032$.

In an experimental setup, we do not expect two stable currents to be distinguishable. Indeed, a current measurement of the SSET-resonator system will yield a weighted average⁶⁴ because decoherence effects will lead to a switching between the two stable configurations on time scales large compared to the oscillation period but small compared to the measurement resolution.⁶⁰ These switching rates can easily be inferred from a comparison of the measured current to the two stable values and from the current noise, as we shall show in section V.

V. NOISE PROPERTIES

A. Charge noise

In the past, linear-response arguments⁹ have been used to support the idea that a generic detector acts on the resonator in the same way as a second thermal bath, and that the backaction on the resonator caused by charge

uctuations on the island can be described essentially by two parameters, a damping rate γ_e and an effective temperature $k_B T_e$. These are related to the charge-noise spectrum

$$S_n(\omega) = \int_{-\infty}^{\infty} dt e^{i\omega t} \langle \dot{n}(t) \dot{n}(0) \rangle \quad (46)$$

via

$$\gamma_e(\omega) = A^2 \frac{S_n(\omega) - S_n(-\omega)}{2\omega}; \quad (47)$$

$$T_e(\omega) = A^2 \frac{S_n(\omega) + S_n(-\omega)}{2\gamma_e(\omega)}; \quad (48)$$

in the limit $k_B T_e(\omega) \rightarrow 0$, where ω is given in units of Γ , $T_e = k_B T_e / \hbar \Gamma$ and $\gamma_e = \gamma_e / \Gamma$. Since these expressions follow from a linear-response calculation, both effective quantities are written in terms of the bare charge-noise, calculated in the absence of coupling with the oscillator.

Investigating the retarded and advanced (absorption and emission) contribution of the charge correlation explicitly, we can derive analytic expressions for $S_n(\omega)$ for the uncoupled SSET (see Appendix D)

$$\begin{aligned} \frac{S_n(\omega) - S_n(-\omega)}{2\omega} &= 2\text{Im}j\omega^2 + M^2 \Gamma^{-1} K_- j\omega; \\ \frac{S_n(\omega) + S_n(-\omega)}{2} &= 2\text{Re}j\omega^2 + M^2 \Gamma^{-1} (K_+ - \text{Im}j\omega) j\omega; \end{aligned} \quad (49)$$

where M denotes again the evolution matrix of the SSET system, $j\omega$ is defined such that $\text{Im}j\omega = \text{Im}\omega$ and K denote coupling matrices given explicitly in Eqs. (C5) and (C6). Note that $\text{Im}j\omega^2 = \text{Im}\omega^2$, $\text{Im}j\omega = \text{Im}\omega$ and K acts only on the off-diagonal elements of $\hat{\rho}_{kj}$, i.e. the Cooper pair tunneling terms.

The self-consistency equation for $\langle \dot{n}^2 \rangle$, that has to be solved in the Gaussian approximation, can be written as

$$\langle \dot{n}^2 \rangle = \frac{2\gamma_{\text{ext}}T_B + 2S_{\text{SSET}}T_{\text{SSET}}(\omega; \omega^2)}{\gamma_{\text{ext}} + S_{\text{SSET}}(\omega; \omega^2)}; \quad (51)$$

where

$$S_{\text{SSET}}(\omega; \omega^2) = i(2A)^2 \quad (52)$$

$$\begin{aligned} \text{Im}j\omega &= \gamma_{\text{ext}}(\gamma_{\text{ext}} + M) \Gamma^{-1} + \gamma_{\text{ext}}M + M^2 \Gamma^{-1} K_- j\omega; \\ 2S_{\text{SSET}}T_{\text{SSET}}(\omega; \omega^2) &= (2A)^2 \quad (53) \end{aligned}$$

$$\text{Im}j\omega_{\text{ext}} + M \Gamma^{-1} + \gamma_{\text{ext}}M + M^2 \Gamma^{-1} K_+ - \text{Im}j\omega; j\omega;$$

We observe that the mean-field equation in second order provides the same physics as linear-response theory, i.e. γ_e at $\omega = 0$ is of the same form as S_{SSET} . Since Eq. (51) is a self-consistency equation for $\langle \dot{n}^2 \rangle$ and not for the effective oscillator energy as in Eqs. (47) and (48) the expressions differ by a factor of 4. The result in Eq. (51) is more accurate in the sense that

the parameters of the damped oscillator are involved: $1 + \gamma_{\text{ext}}M + M^2 = 1 - (\gamma_{\text{ext}}/2)^2 + \frac{M + \gamma_{\text{ext}}/2}{2} (\gamma_{\text{ext}}/2)^2$ with a renormalized frequency of $\omega_r = \frac{M + \gamma_{\text{ext}}/2}{2} (\gamma_{\text{ext}}/2)^2$ and additional damping due to $\gamma_{\text{ext}}/2$.

Note that Eq. (51) is a self-consistency equation for $\langle \dot{n}^2 \rangle$ since $j\omega = j(\omega; \omega^2)$ and it has to be solved together with $\langle \dot{n} \rangle = 2A\text{Im}j\omega$. Even if it is assumed that $j\omega = j(0; 2T_B)$, the expression contains a correction due to the finite quality factor of the NR.

Whereas the approach describing the detector as an effective bath proved very successful in providing a simple physical explanation of experiments,¹⁰ some of its shortcomings have started to be identified in recent theoretical works.^{61,62} For example, it has very recently been proposed⁶² that the signature of the oscillator in the charge noise spectrum of a generic detector is not the one of a thermal oscillator. In the light of these findings, the calculation of the full frequency-dependent charge noise spectrum of the SSET near the DJQP in the presence of an oscillator becomes relevant, even more so since the charge-noise spectrum is an experimentally accessible quantity.

As shown in Appendix D, it is possible to use the master-equation approach to derive formal expressions for $S_n(\omega)$, at least for weak coupling in the thermal-oscillator approximation. However, it turns out that these expressions are difficult to evaluate explicitly for stronger couplings (in the Gaussian approximation). On the other hand, the fully numerical approach presented in section IIC can easily be adapted to allow the calculation of finite-frequency correlation functions of system (as opposed to bath) operators, using the quantum regression theorem.^{63,64} In the following, we therefore discuss only the charge-noise spectrum obtained numerically. Note that we verified that our algorithm reproduces accurately the known charge and position fluctuation spectra in the uncoupled ($A = 0$) regime.

Figure 9 shows the symmetrized (in frequency) charge-noise spectra, $S_n^{\text{sym}}(\omega) = [S_n(\omega) + S_n(-\omega)]/2$, obtained for different values of the bias-voltage detuning from the DJQP resonance. The oscillator state, i.e. thermal or driven, can be determined from the Fock space probability distribution in Fig. 5. The inset shows that the signature of the oscillator in $S_n^{\text{sym}}(\omega)$ appears prominently around the natural frequency of the oscillator. Away from $\omega = 0$, the charge spectrum is only weakly affected by the oscillator, since the coupling of the island to the resonator changes the effective biasing conditions of the SSET.

The main panel of Fig. 9 shows the evolution of the charge-noise spectra when the system is taken from the "cooling" region ($V = -1$) through the resonance point ($V = 0$), to the voltage regime where the state of the oscillator becomes highly non-thermal. Unsurprisingly, the overall signal around $\omega = 0$ increases dramatically when the oscillator enters the driven regime, reflecting the overall increase in the magnitude of $S_x(\omega)$ when the oscillator's energy is increased. Associated with this increased

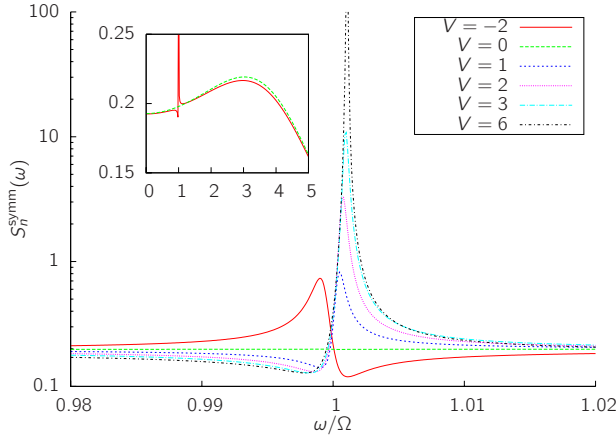


FIG. 9: Frequency-dependent charge noise of the charge n on the SSET, symmetrized contribution $S_n^{\text{sym}}(\omega)$, versus ω/Ω for different values of the bias voltage eV measured from the resonance. Parameters are identical to Fig. 5. While there is no structure in the case $V = 0$, we can distinguish if the oscillator is driven or cooled by the symmetry of the peak at $\omega/\Omega = 1$. Inset: $S_n^{\text{sym}}(\omega)$ in a larger parameter regime; numerical calculation $\tilde{A} = 0.1$ compared to analytical result $\tilde{A} = 0$.

magnitude is an overall reduction of the linewidth, that is again explained rather straightforwardly via the decreased total damping rate in this region ($e < 0$).

The most interesting observation to be made about Fig. 9 is perhaps the striking similarity between the spectra at $V < 0$ and $V = 0$. In both cases, we find not only a resonance at the renormalized frequency of the oscillator, but also a dip at its bare frequency, exactly as derived in Ref. [62] for a generic detector. Note that the renormalized frequency $\omega_r(V) = \frac{\omega}{\sqrt{1 + \frac{e}{\tilde{A}}(V)}}$ depends on the detuning V . For $V < 0$ we find $e > 0$, such that the renormalized frequency ω_r is smaller than ω . In the region $V > 0$ and $e < 0$, the situation is reversed and the resonance appears at frequencies ω_r higher than ω , while the dip is pinned. No structure is observed exactly at $V = 0$ which relates to $e(V = 0) = 0$ since absorption and emission of energy from the SSET to the oscillator at the DJQP resonance is equal.

The presence of a dip is not compatible with a purely "thermal" state of the oscillator, even in cases where the Fock state probability distribution function $P(n_{\text{osc}})$ decays exponentially like in the fully-thermal case [cf. Fig. 5]. Not only does this result confirm that the simple model used in Ref. [62] also applies to the complex SSET-resonator system, it also demonstrates that the "Fano-like" lineshape, where both a resonance and a dip appear in the spectrum of the charge noise, characterizes nicely the charge noise spectrum on both the "driving" and "cooling" sides of the resonance.

B. Current noise

We argued previously that the non-thermal oscillator states (i.e., cooling and driving of the resonator) manifest themselves in the cumulants of coupled system. Therefore, it is reasonable to expect that the coupling with the NR will modify the current fluctuations of the SSET.

In the following, we will focus mainly on the Fano factor, i.e. the current noise at $\omega = 0$ which is easily accessible by standard noise measurement techniques. The frequency-dependent current noise is given by MacDonald's formula⁶⁵

$$S_I(\omega) = \frac{1}{Z} \int_0^Z dt e^{i\omega t} \langle I(t) I(0) \rangle$$

$$= (e^2) \int_0^Z dt \sin(\omega t) \frac{d}{dt} \langle n_R(t) \rangle \quad (54)$$

From this formula, we can deduce the following zero-frequency limit,^{47,64}

$$S_I(\omega \rightarrow 0) = (e^2) \lim_{\omega \rightarrow 0} \frac{d}{dt} \langle n_R(t) \rangle \quad (55)$$

Thus we have to determine the long-time limit of $\frac{d}{dt} \langle n_R(t) \rangle$. Note that we assume for the derivation symmetric capacitances such that $S_{LL}(\omega = 0) = S_{RR}(\omega = 0)$ due to charge conservation.⁴⁴ Since we use the symmetrized current noise, the Fano factor is defined as $F = S_I(\omega = 0) / (e^2 \hbar \omega)$ without a factor of 2.

In order to use Eq. (20) to calculate numerically the current noise, we follow closely the approach presented in Ref. [53]. The original approach which applied to incoherent processes can be generalized to the coherent Josephson tunneling. The zero-frequency current noise is thus given by

$$S_I(\omega \rightarrow 0) = (e^2) \frac{\hbar}{2} \text{Tr}_n \text{Tr}_{\text{osc}} (I_{\text{noise}} \text{stat})$$

$$= \frac{1}{2} \text{Tr}_n \text{Tr}_{\text{osc}} (I_{\text{total}} R I_{\text{total}} \text{stat}) \quad (56)$$

where $I_{\text{total}} = I_{\text{qp}} + 2I_{\text{CP}}^+ + 2I_{\text{CP}}^-$ is the superoperator describing the total current as defined previously, $I_{\text{noise}} = I_{\text{qp}} + 4I_{\text{CP}}^+ + 4I_{\text{CP}}^-$ and R is the pseudoinverse of the Liouvillian L .⁶⁴ We compared both the Fano factor and the frequency-dependent current noise in the uncoupled case with the exact expressions of Ref. 43 (see also App. E) and verified thus the correctness of Eq. 56).

As in the previous section it is possible to obtain an analytic expression in the thermal-oscillator approximation. For details of the calculation we refer to Appendix E. We find

$$F = \frac{3}{2} + \frac{3}{2} \frac{f_{\text{sym}} + f_{\text{asym}}}{\frac{1}{\tilde{\omega}_L} + \frac{1}{\tilde{\omega}_R} + \frac{1}{\omega_L} + \frac{1}{\omega_R}} \quad (57)$$

The term

$$f_{\text{sym}} = 3 \left(\frac{1}{\tilde{\omega}_L} + \frac{1}{\tilde{\omega}_R} \right) \left(\frac{1}{\omega_L} + \frac{1}{\omega_R} \right) \quad (58)$$

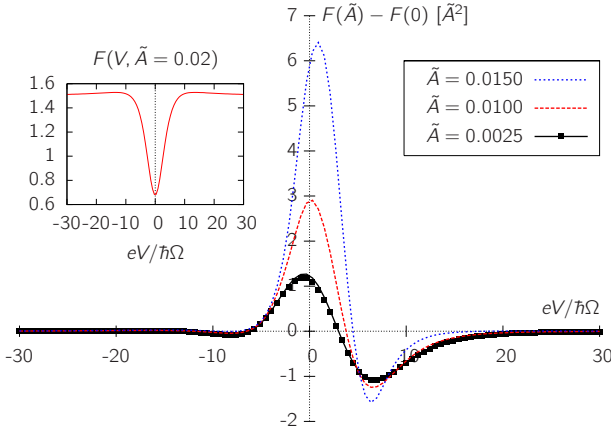


FIG. 10: Difference in Fano factors $F = F(\tilde{A}) - F(\tilde{A} = 0)$ in units of \tilde{A}^2 as a function of bias voltage $eV = \hbar\Omega$ for $\tilde{\gamma}_L = \tilde{\gamma}_R = 10$, $J_L = J_R = 2$, $\gamma_{\text{ext}} = 0.0001$ and $T_B = 2.5$. Lines depict results of the numerical approach. The results of the Gaussian approximation (points) quantitatively only for $\tilde{A} < 0.01$. Inset: the Fano factor $F(\tilde{A} = 0.02)$ decreases at $V = 0$ when the Cooper pair tunneling is resonant.

reduces the noise^{41,66} at the resonance; this is a consequence of the coherence of the Cooper pair tunneling. The asymmetric part

$$f_{\text{asym}} = \frac{1}{\tilde{\gamma}_L} \frac{1}{\tilde{\gamma}_R} + \frac{1}{\tilde{\gamma}_L} \frac{1}{\tilde{\gamma}_R} + \frac{1}{\tilde{\gamma}_L} \frac{1}{\tilde{\gamma}_R} + \frac{1}{\tilde{\gamma}_L} \frac{1}{\tilde{\gamma}_R} + \frac{1}{\tilde{\gamma}_L} \frac{1}{\tilde{\gamma}_R} + \frac{1}{\tilde{\gamma}_L} \frac{1}{\tilde{\gamma}_R} + \frac{1}{\tilde{\gamma}_L} \frac{1}{\tilde{\gamma}_R} + \frac{1}{\tilde{\gamma}_L} \frac{1}{\tilde{\gamma}_R} \quad (59)$$

increases the noise level, for example if the coupling is asymmetric, $\tilde{\gamma}_L \neq \tilde{\gamma}_R$, or the system is tuned away from the resonance, i.e. $\tilde{\gamma}_L \neq 0$ or $\tilde{\gamma}_R \neq 0$.

The coupling of the SSET and the NR enters via the $\hbar\omega$ dependence of the Cooper pair tunneling rates $\tilde{\gamma}_L(\omega)$ and $\tilde{\gamma}_R(\omega)$ defined in Eqs. (41) and (42). In the thermal oscillator approximation the effect is thus of second order in \tilde{A} as observed already for the current. In analogy to the previous section the coupling of the SSET to the NR leads in the thermal approximation only to a shift in the resonance position of the SSET. Since the resonance condition is important for coherent Cooper pair tunneling, the shift manifests itself in a higher noise signal around $V = 0$, leading to a peak in $F = F(\tilde{A} \neq 0) - F(\tilde{A} = 0)$, see Fig. 10. At large voltages both the Fano factor of the coupled and uncoupled SSET converge to the value $3/2$.

In order to access the regime of increased coupling, we investigated the current noise also in the Gaussian approximation and compared the result to the numerical calculation explained below. For very low coupling up to $\tilde{A} = 0.01$, as long as the resonator remains close to its thermal state, the two approximations coincide. For increased coupling, however, deviations from the effective backgate behavior appear. A plot of the difference in Fano factors F as a function of the bias voltage is shown in Fig. 10.

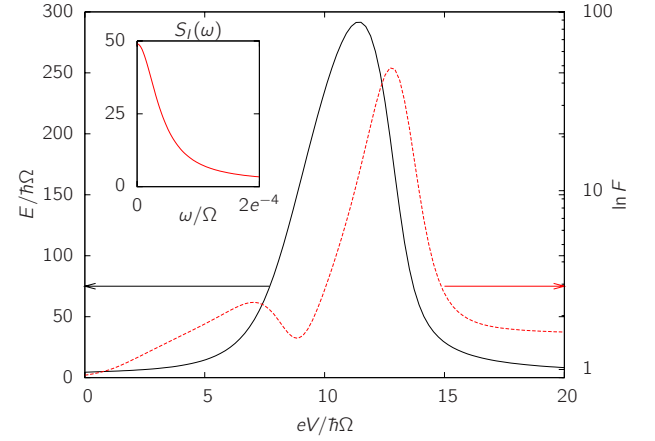


FIG. 11: Logarithmic Fano factor $\ln F$ and oscillator energy $E = \hbar\Omega$ as a function of bias voltage $eV = \hbar\Omega$. The parameters are $eV_G = \hbar\Omega = 2.5$; $\tilde{\gamma}_L = \tilde{\gamma}_R = 12$, $J_L = J_R = 2.5$, $\gamma_{\text{ext}} = 0.001$, $T_B = 3$, and $\tilde{A} = 0.1$. The Fano factors shows a first peak when the system enters the driven state. At the onset of the bistability, the Fano factor increases drastically on the logarithmic scale, which we attribute to telegraph noise due to switching between the two stable configurations. Inset: frequency-dependent current noise in the bistable region ($eV = \hbar\Omega = 12.8$) which decays on the scale of the switching rates.

We find that the central peak in F is accompanied by two negative side peaks where the current noise of the coupled SSET is lower than the uncoupled value. In the cooling and driving regimes the SSET absorbs and emits energy to the resonator in order to move closer to the resonance position. As pointed out before, the noise at the resonance is reduced due to the coherent Cooper pair tunneling and therefore the cooling and driving mechanisms are responsible for the negative side peaks. As in the energy of the resonator, Fig. 6, the driving is stronger than the cooling, which manifests itself in the heights of the negative side peaks.

Even before the bistability arises, the coupling between the SSET and the NR leads to a modification of the current noise, from which one can deduce if (and to which extent) the oscillator is cooled or driven.

In the bistable regime, the master equation approach leads to two solutions for the noise corresponding to the two stable solutions for the current. We argued previously that in this regime, a thermal and a driven solution coexist. Experimentally, however, the two solutions will not be completely stable and the system will switch between the two states on a time scale much slower than the other system time scales. As was shown generally for bistable systems^{53,54} and was also recovered for the case of the JQP,⁴⁰ the experimentally measured noise will then be dominated by the switching between the two stable states and will then essentially be telegraph noise. This type of low-frequency noise is most clearly visible in the Fano factor which we have evaluated using the numerical approach in Fig. 11.

The Fano factor first peaks roughly at the transition between the thermal state and the driven state. It then descends to a local minimum. This behavior is correlated to the stationary value of the average position of the oscillator, $\langle x \rangle$, which acts as an effective backgate on the SSET as discussed in detail in connection with Fig. 10. In the driven state the transfer of energy from the SSET to the NR is maximal and therefore we observe a minimum in the Fano factor. Beyond the pure driven state, the system reaches the bistable region which clearly shows up as a drastically increased Fano factor on the logarithmic scale in Fig. 11. We attribute this zero-frequency noise feature to a slow switching between the two stable configurations of the system.⁴⁰

The inset of Fig. 11 shows the frequency-dependence of the current noise at the voltage where the Fano factor is maximal. As expected for a bistable system the value drops fast from the superpoissonian value on a scale given by the sum of the two switching rates⁶⁴, which are very slow compared to the other scales of the system. In the frequency-dependent current noise [not explicitly shown here] we find signatures at the frequency of the oscillator and at higher harmonics, which appear as a thermal resonance on top of the uncoupled current noise of the SSET.

VI. CONCLUSIONS

In conclusion, we have provided a comprehensive treatment of a superconducting single-electron transistor capacitively coupled to a nanomechanical resonator. Assuming a linearized coupling for typical system parameters, we have found that signatures of the mutual interaction manifest themselves as well in physical quantities related to the oscillator as in the current and noise properties of the transistor.

It is known that this setup with the SSET close to the resonance condition for the double Josephson quasiparticle process is especially suitable to cool the oscillator or drive it. We confirm this behavior and explain how the different approximations fail or succeed in capturing these features. We use two complementary approaches, a purely numerical solution of the Liouville equation and a mean-field analysis, which lead to identical results in the accessible parameter region. In addition to driving effects of the oscillator, our solution predicts the emergence of a bistable regime for increased coupling.

Although the consequences of cooling and driving the resonator have been studied in previous work, the questions of if and how these non-thermal states can be measured in the transport properties of the coupled SSET close to the DJQP resonance were not discussed in the literature. This obvious gap is addressed in our work. We find that the current through the SSET gives a measure of the displacement of the oscillator since, at the lowest-order, the coupling with the NR modifies the gating condition of the SSET.

Investigating the fluctuations close to the resonance frequency of the mechanical oscillator, we find pronounced effects. For instance, the frequency-resolved charge noise shows a sharp resonance/dip structure close to the resonator frequency, which allows to estimate the sign of the effective damping. Moreover, we have studied the zero-frequency current noise, i.e. the Fano factor. Depending on the applied voltages, the SSET coupled to an NR results in an increase or decrease of the Fano factor compared to the uncoupled case. We could show that a decrease is related to driving or cooling of the NR. Furthermore we find that the Fano factor increases notably as soon as the system enters the bistable state. This feature can be used experimentally to pinpoint the bistable region. The switching rates between the two stable regimes can be identified from the frequency dependence of the current noise.

In comparison to an SSET driven at a JQP resonance, the DJQP shows stronger effects for lower couplings. Extending the parameter regime to strong coupling, different methods have to be applied and also the assumption of a linear coupling is challenged. This will be the subject of future work.

Acknowledgments

We would like to thank A.D.Armour and C.Flinn for interesting discussions and M.S.Choi for his support. This work was financially supported by the Swiss NSF and the NCCR Nanoscience.

APPENDIX A: COUPLING OF SSET AND NR

The coupling between the SSET and the NR originates from a capacitive coupling between the island with the gated resonator. The displacement x , i.e. the deviation from the equilibrium distance d , determines the capacitance $C_N(x)$

$$C_N(x) = C_N^0 \frac{A}{x+d} = C_N^0 \frac{x=d}{1+x=d}; \quad (\text{A } 1)$$

and thus the charging energy E_C and the charge on the island n_0

$$\begin{aligned} E_C(x) &= \frac{e^2}{2} \frac{1}{C_L + C_R + C_G + C_N(x)} \\ &= E_C^0 \frac{1}{1 + \frac{C_N^0}{C} \frac{x=d}{1+x=d}}; \end{aligned} \quad (\text{A } 2)$$

$$\begin{aligned} n_0(x) &= \frac{1}{e} (C_L V_L + C_R V_R + C_G V_G + C_N(x) V_N) \\ &= n_0^0 \frac{C_N^0 V_N}{e} \frac{x=d}{1+x=d}; \end{aligned} \quad (\text{A } 3)$$

such that

$$2 \frac{eV^{DJQP}}{\sim} = \frac{4E_C}{\sim}; \quad (B7)$$

and we denote any shift away from V^{DJQP} as V . Consequently the energy detuning is given by the gate and bias voltage as

$$1; 1 = 2 \frac{C_G}{C} \frac{eV_G}{\sim} + \frac{eV}{\sim} \mathcal{A}^{\text{hxi}}; \quad (B8)$$

$$2; 0 = 2 \frac{C_G}{C} \frac{eV_G}{\sim} - \frac{eV}{\sim} \mathcal{A}^{\text{hxi}}; \quad (B9)$$

For convenience only, it is assumed in the calculations that $eV_G = \sim$ and $eV = \sim$ have the same prefactors (see Eqs. (43) and (44)) and for abbreviation also is mostly skipped.

In the stationary limit, i.e. $d\langle \pi \rangle / dt = 0$, we find immediately

$$\langle \pi \rangle = iJ_L M^{-1} \langle \pi \rangle; \quad (B10)$$

or written down explicitly

$$\langle \pi \rangle = \frac{1}{2} \left(\frac{1}{R} + \frac{1}{L} + \frac{1}{\sim_R} + \frac{1}{\sim_L} \right)^{-1} \left(i\tilde{J}_R \frac{2}{\sim_R} \frac{1}{\frac{\sim_L}{2} + i1; 1} + i\tilde{J}_R \frac{2}{\sim_R} \frac{1}{\frac{\sim_L}{2} - i1; 1} + i\tilde{J}_L \frac{2}{\sim_L} \frac{1}{\frac{\sim_R}{2} + i2; 0} + i\tilde{J}_L \frac{2}{\sim_L} \frac{1}{\frac{\sim_R}{2} - i2; 0} \right); \quad (B11)$$

This result can be inserted in Eqs. (38) and (39) and we find the result for the current hI , Eq. (40).

Note that $hI^{ND} = 2hI^D$ follows immediately from the equation (B2)

$$\frac{d}{dt} \langle \pi_{11} \rangle = i\tilde{J}_R \langle \pi_{1; 1} \rangle - \langle \pi_{1; 1} \rangle + \sim_R \langle \pi_{2; 2} \rangle \quad (B12)$$

in the stationary limit. This expression is due to the nature of the DJQP process and does not change if we go to more sophisticated approximations.

The shift of the oscillator resonance is proportional to the charge on the island,

$$\begin{aligned} m_i &= 2\langle \pi_{2; 2} \rangle + \langle \pi_{1; 1} \rangle - \langle \pi_{1; 1} \rangle \\ &= \frac{1}{R} + \frac{1}{\sim_R} = \frac{1}{R} + \frac{1}{L} + \frac{1}{\sim_R} + \frac{1}{\sim_L} \\ &= \frac{1}{R} + \frac{1}{\sim_R} \frac{2hI}{3(e)}; \end{aligned} \quad (B13)$$

As obvious from Eq. (40) the slowest rate limits the current and thus determines its value. In the symmetric case $J_L = J_R = J$ and $\sim_L = \sim_R = \sim$ the current can also be written more explicitly in terms of the system parameters⁵⁹

$$hI = (e) \frac{6\sim^2}{2\frac{\sim^2}{2; 0} + 2\frac{\sim^2}{1; 1} + 8J^2 + \sim^2}; \quad (B14)$$

As discussed in the main text the shift due to the coupling to the leads can be read off from

$$\begin{aligned} \frac{3(e)}{2} \frac{1}{hI} &= \frac{1}{hI(\mathcal{A} = 0)} \\ &= \frac{1}{L(\mathcal{A})} + \frac{1}{L(\mathcal{A} = 0)} + \frac{1}{R(\mathcal{A})} + \frac{1}{R(\mathcal{A} = 0)}; \end{aligned} \quad (B15)$$

In the symmetric case $J_L = J_R = J$ and $\sim_L = \sim_R = \sim$ as assumed in the main text, this can be written more explicitly as

$$\begin{aligned} \frac{3(e)}{2} \frac{1}{hI} &= \frac{1}{hI(\mathcal{A} = 0)} \\ &= 2(2\mathcal{A}^{\text{hxi}})^{-1} \frac{eV_G}{\sim}; \end{aligned} \quad (B16)$$

Since \mathcal{A}^{hxi} depends on the bias voltage V , the value of $2\mathcal{A}^{\text{hxi}}(V; V_G)$ can be extracted from the intersection with the voltage axis when plotting $1/hI(\mathcal{A}) - 1/hI(\mathcal{A} = 0)$.

APPENDIX C: MEAN-FIELD EQUATIONS FOR GAUSSIAN APPROXIMATION

In the thermal-oscillator approximation we assumed that $\langle \pi_{xii} \rangle = \langle \pi_{vii} \rangle = 0$. For stronger coupling, the accuracy of this assumption gets worse and we proceed to calculate $\langle \pi_{xii} \rangle = \langle \pi_{jxpii} \rangle$ with $\langle \pi_{jj} \rangle = (1; 1; 0; 0; 2; 0; 0)$ in the Gaussian approximation. Here $\langle \pi_{jxpii} \rangle$ denotes the vector of cumulants $\langle \pi_{jxpii} \rangle = \langle \pi_{jxpii} \rangle - \langle \pi_{jxpii} \rangle \langle \pi_{jxpii} \rangle$. Higher-order expectation values are assumed to vanish, for example from $\langle \pi_{x^2 jxpii} \rangle = 0$ it follows that

$$x^2 \langle \pi_{jxpii} \rangle = 2\langle \pi_{jxpii} \rangle \langle \pi_{jxpii} \rangle + x^2 \langle \pi_{jxpii} \rangle; \quad (C1)$$

This approximation leads us to the following set of equations:

$$\frac{d}{dt} \langle \pi \rangle = M \langle \pi \rangle + i\tilde{J}_L \langle \pi \rangle + 2i\mathcal{A}K \langle \pi_{jxpii} \rangle; \quad (C2)$$

$$\frac{d}{dt} \langle \pi_{jxpii} \rangle = M \langle \pi_{jxpii} \rangle + \langle \pi_{jxpii} \rangle + 2\mathcal{A}K^2 \langle \pi \rangle; \quad (C3)$$

$$\begin{aligned} \frac{d}{dt} \langle \pi_{jvpii} \rangle &= M \langle \pi_{jvpii} \rangle - \langle \pi_{jvpii} \rangle + \text{ext} \langle \pi_{jvpii} \rangle \\ &\quad + 2\mathcal{A}(K + m_i) \langle \pi \rangle; \end{aligned} \quad (C4)$$

where the coupling matrices are given by

$$K_+ = \text{diag} (1; 1; 0; 0; 2; 1; 1); \quad (\text{C } 5)$$

$$K_- = \text{diag} (0; 0; 1; 1; 0; 1; 1); \quad (\text{C } 6)$$

This set of equations can be solved in the stationary limit and is given here in matrix representation

$$\dot{\mathbf{p}} = i\tilde{J}_L \mathbf{M} + i(2\tilde{A})^2 K_-^{-1} + \tilde{\gamma}_{\text{ext}} \mathbf{M} + \mathbf{M}^2 \mathbf{K}_+^{-1} (\mathbf{K}_+ - \mathbf{M}) + i\mathbf{h}^2 \mathbf{ii} (\tilde{\gamma}_{\text{ext}} + \mathbf{M}) \mathbf{K}_+^{-1} \mathbf{p}; \quad (\text{C } 7)$$

$$\dot{\mathbf{j}} \mathbf{p} \mathbf{ii} = 2\tilde{A}^{-1} + \tilde{\gamma}_{\text{ext}} \mathbf{M} + \mathbf{M}^2 \mathbf{K}_+^{-1} (\mathbf{K}_+ - \mathbf{M}) + i\mathbf{h}^2 \mathbf{ii} (\tilde{\gamma}_{\text{ext}} + \mathbf{M}) \mathbf{K}_+^{-1} \mathbf{p}; \quad (\text{C } 8)$$

Since in the stationary limit

$$\mathbf{M} \mathbf{j} \mathbf{p} \mathbf{ii} = \mathbf{M} \mathbf{j} \mathbf{p} \mathbf{ii} \quad (\text{C } 9)$$

we do not need to calculate $\mathbf{h} \mathbf{v} \mathbf{ii}$ and find instead

$$\mathbf{h} \mathbf{x}^2 \mathbf{ii} = \mathbf{h} \mathbf{v}^2 \mathbf{ii} + 2\tilde{A} \mathbf{M} \mathbf{j} \mathbf{p} \mathbf{ii} = 2\tilde{T}_B + 2\tilde{A} \tilde{\gamma}_{\text{ext}} \mathbf{M} \mathbf{j} \mathbf{p} \mathbf{ii} + 2\tilde{A} \mathbf{M} \mathbf{j} \mathbf{p} \mathbf{ii}; \quad (\text{C } 10)$$

Using the general solution for $\mathbf{j} \mathbf{p} \mathbf{ii}$ we can rewrite this equation with the expression

$$\mathbf{h} \mathbf{x}^2 \mathbf{ii} = \frac{2\tilde{\gamma}_{\text{ext}} \tilde{T}_B + 2 \text{SSET } T_{\text{SSET}}(\mathbf{x}; \mathbf{x}^2)}{\tilde{\gamma}_{\text{ext}} + \text{SSET }(\mathbf{x}; \mathbf{x}^2)}; \quad (\text{C } 11)$$

where we define

$$\begin{aligned} \text{SSET }(\mathbf{x}; \mathbf{x}^2) &= i(2\tilde{A})^2 \mathbf{h} \mathbf{j} \mathbf{1} - \tilde{\gamma}_{\text{ext}} (\tilde{\gamma}_{\text{ext}} + \mathbf{M})^{-1} + \tilde{\gamma}_{\text{ext}} \mathbf{M} + \mathbf{M}^2 \mathbf{K}_+^{-1} \mathbf{p}(\mathbf{x}; \mathbf{x}^2) \mathbf{i}; \\ 2 \text{SSET } T_{\text{SSET}}(\mathbf{x}; \mathbf{x}^2) &= (2\tilde{A})^2 \mathbf{h} \mathbf{j} \tilde{\gamma}_{\text{ext}} + \mathbf{M}^{-1} + \tilde{\gamma}_{\text{ext}} \mathbf{M} + \mathbf{M}^2 \mathbf{K}_+^{-1} \mathbf{K}_+ - \mathbf{M} \mathbf{i} \mathbf{p}(\mathbf{x}; \mathbf{x}^2) \mathbf{i}; \end{aligned}$$

The equation for $\mathbf{h} \mathbf{x}^2 \mathbf{ii}$ has to be solved together with the expression for $\mathbf{h} \mathbf{x} \mathbf{i}$ which leads in some parameter regime to more than one solution. This bistability of the model is discussed in detail in the main text.

APPENDIX D: CHARGE NOISE OF THE SSET

To calculate the charge noise in the DQJP we evaluate the expression

$$\begin{aligned} S_n(\omega) &= \frac{1}{Z} \int_{-1}^1 dt e^{i\omega t} \mathbf{h} \mathbf{n}(t) \mathbf{n}(0) \mathbf{ii} \quad (\text{D } 1) \\ &= \frac{1}{Z} \int_{-1}^1 dt \cos(\omega t) \mathbf{h} \mathbf{n}(t) \mathbf{n}(0) \mathbf{ii} + \mathbf{h} \mathbf{n}(-t) \mathbf{n}(0) \mathbf{ii} \\ &\quad + i \frac{\omega}{Z} \int_0^1 dt \sin(\omega t) \mathbf{h} \mathbf{n}(t) \mathbf{n}(0) \mathbf{ii} - \mathbf{h} \mathbf{n}(-t) \mathbf{n}(0) \mathbf{ii} \end{aligned}$$

and take into account that $S_n(t)$ is not necessarily symmetric. Therefore we introduce two new functions⁶⁶

$$\langle \mathbf{n} \rangle = \text{Tr}_{\text{osc}} \text{Tr}_{n_R} f e^{i\mathbf{H} t} \mathbf{n} e^{-i\mathbf{H} t} \mathbf{g}; \quad (\text{D } 2)$$

$$\langle \mathbf{n} \rangle = \text{Tr}_{\text{osc}} \text{Tr}_{n_R} f e^{i\mathbf{H} t} \mathbf{n} e^{-i\mathbf{H} t} \mathbf{g}; \quad (\text{D } 3)$$

The partial traces are taken over the oscillator degree of freedom and the tunneled charge n_R . These functions

have the properties $\mathbf{h} \mathbf{n}(t) \mathbf{n}(0) \mathbf{ii} = \text{Tr}_{n_R} f \mathbf{n}(t) \mathbf{g} \mathbf{h} \mathbf{n}^2$ and $\mathbf{h} \mathbf{n}(-t) \mathbf{n}(0) \mathbf{ii} = \text{Tr}_{n_R} f \mathbf{n}(t) \mathbf{g} \mathbf{h} \mathbf{n}^2$ where Tr_{n_R} denotes the trace of the charge states of the island. The functions $\langle \mathbf{n} \rangle$ and $\langle \mathbf{n} \rangle$ fulfill the same differential equation

$$\frac{d}{dt} \mathbf{j} \mathbf{i} = -\mathbf{M} \mathbf{j} \mathbf{i} + i\tilde{J}_L \mathbf{h} \mathbf{n} \mathbf{i} \mathbf{j} \mathbf{i}; \quad (\text{D } 4)$$

$$\frac{d}{dt} \mathbf{j} \mathbf{i} = -\mathbf{M} \mathbf{j} \mathbf{i} + i\tilde{J}_L \mathbf{h} \mathbf{n} \mathbf{i} \mathbf{j} \mathbf{i}; \quad (\text{D } 5)$$

with different initial conditions

$$\mathbf{j}(0) \mathbf{i} = \text{Tr}_{\text{osc}} \text{Tr}_{n_R} f \mathbf{n} \mathbf{g} = \mathbf{K} \mathbf{p} \mathbf{i}; \quad (\text{D } 6)$$

$$\mathbf{j}(0) \mathbf{i} = \text{Tr}_{\text{osc}} \text{Tr}_{n_R} f \mathbf{n} \mathbf{g} = \mathbf{K} \mathbf{p} \mathbf{i}; \quad (\text{D } 7)$$

where $\mathbf{K} = \mathbf{K}_+ + \mathbf{K}_-$ and $\mathbf{K} = \mathbf{K}_+ - \mathbf{K}_-$. Straightforwardly we find

$$\mathbf{h} \mathbf{n}(t) \mathbf{n}(0) \mathbf{ii} + \mathbf{h} \mathbf{n}(-t) \mathbf{n}(0) \mathbf{ii} = 2 \mathbf{h} \mathbf{n} e^{\mathbf{M} t} (\mathbf{K}_+ - \mathbf{M}) \mathbf{p} \mathbf{i}$$

$$\mathbf{h} \mathbf{n}(t) \mathbf{n}(0) \mathbf{ii} - \mathbf{h} \mathbf{n}(-t) \mathbf{n}(0) \mathbf{ii} = 2 \mathbf{h} \mathbf{n} e^{\mathbf{M} t} \mathbf{K} \mathbf{p} \mathbf{i}; \quad (\text{D } 8)$$

and consequently

$$\begin{aligned} S_n(\omega) &= 2 \mathbf{h} \mathbf{j} \frac{\mathbf{M}}{(\omega^2 + \mathbf{M}^2)} (\mathbf{K}_+ - \mathbf{M}) \mathbf{p} \mathbf{i} \\ &\quad + 2i \mathbf{h} \mathbf{j} \frac{(\omega^2 - \mathbf{M}^2)}{(\omega^2 + \mathbf{M}^2)} \mathbf{K} \mathbf{p} \mathbf{i}; \quad (\text{D } 9) \end{aligned}$$

For example the effective damping and temperature in linear-response theory is related to

$$\frac{S_n(\omega) - S_n(-\omega)}{2(\omega = \gamma)} = 2\hbar n_j \frac{1}{(\omega = \gamma)^2 + M^2} K_{ij} \quad (E10)$$

$$\frac{S_n(\omega) + S_n(-\omega)}{2} = 2\hbar n_j \frac{M}{(\omega = \gamma)^2 + M^2} (K_{ij} + \text{Im}i) \quad (E11)$$

as is discussed in more detail in the main text. Note the striking similarity to the self-consistency equation for the Gaussian approximation, Eqs. (51-54).

APPENDIX E: CALCULATION OF THE CURRENT NOISE

We want to calculate $d\langle n_R^2 \rangle/dt$ and study therefore the time-evolution of

$$\begin{aligned} d\langle n_R^2 \rangle/dt &= \text{Tr} \left[\frac{d}{dt} \rho_R(t) n_R^2 \right] \\ &= \frac{i}{\hbar} \text{Tr} \left[(n_R + n_R^\dagger) [H_R, n_R^2] \right] \end{aligned} \quad (E1)$$

Therefore we introduce the n_R -resolved density matrix. Defining the operator

$$\rho_{kj}^{n_R, m_R} = \text{Tr}_{\text{osc}} \text{Tr}_{n_R} \text{Tr}_{n_R^\dagger} \rho_{ij} \rho_{kj}^{n_R, m_R} \quad (E2)$$

such that $\rho_{kj}^{n_R, m_R} = \text{Tr}_{\text{osc}} \text{Tr}_{n_R} \text{Tr}_{n_R^\dagger} \rho_{ij} \rho_{kj}^{n_R, m_R}$ and $\rho_{kj}^{n_R, m_R} = \text{Tr}_{\text{osc}} \text{Tr}_{n_R} \text{Tr}_{n_R^\dagger} \rho_{ij} \rho_{kj}^{n_R, m_R}$. Note that $\rho_{kj}^{n_R, m_R}$ is a different quantity since n_R and $\rho_{kj}^{n_R, m_R}$ do not commute.

We assume the stationary limit in the sense that $\rho_{kj}^{n_R, m_R}$ does not depend on time. Then, the n_R -resolved density operator can be calculated in the thermal-oscillator approximation where the differential equation reads

$$\frac{d}{dt} \rho_{kj}^{n_R, m_R}(t) = -M \rho_{kj}^{n_R, m_R} + \mathcal{A}_{ij} + \text{Im}i \rho_{kj}^{n_R, m_R} \quad (E3)$$

$$\mathcal{A}_{ij} = \begin{pmatrix} 0 & 2i\tilde{\gamma}_R \rho_{1,1}^i & 1 \\ \tilde{\gamma}_R \rho_{22}^i + 2i\tilde{\gamma}_R \rho_{1,1}^i & 2i\tilde{\gamma}_R \rho_{1,1}^i & 0 \\ 2i\tilde{\gamma}_R \rho_{1,1}^i & 2i\tilde{\gamma}_R \rho_{1,1}^i & 0 \\ 0 & 0 & 0 \end{pmatrix} \quad (E4)$$

since $(-e)\hbar n_i = \hbar i$ it is explicitly time-dependent (in the stationary limit $\hbar i(t) = \hbar i$), the differential equation has to be solved explicitly and we find

$$\begin{aligned} \rho_{R,pii}(\tau) &= e^{-M\tau} \rho_{R,p}(\tau=0) \\ &+ (1 - e^{-M\tau}) M^{-1} \mathcal{A}_{ii} \frac{\hbar i}{(-e)} M^{-1} \rho_{ij} \end{aligned} \quad (E5)$$

Note that $\rho_{R,pii}$ denotes similarly to previous definitions the vector of finite $\rho_{R,p_{kj}i}$ and $\rho_{R,pii} = \rho_{R,pii}$.

The noise itself has a structure similar to the current, but with some correction terms from the counting of n_R

$$\hbar i = (-e)\hbar \rho_{ij} \quad (E6)$$

$$d\langle n_R^2 \rangle/dt = 2(-e)^2 \hbar \rho_{R,pii} + (-e)^2 \tilde{\gamma}_R \rho_{22}^i \quad (E7)$$

$$2(-e)^2 2i\tilde{\gamma}_R \rho_{1,1}^i + \rho_{1,1}^i \quad (E8)$$

$$\hbar j = \begin{pmatrix} 0 & 0 & 2i\tilde{\gamma}_R & 2i\tilde{\gamma}_R & \tilde{\gamma}_R & 0 & 0 \end{pmatrix} \quad (E8)$$

If we apply MacDonald's formula⁶⁵ for the symmetrized noise, i.e. $S_I(t) = S_I(-t)$, we find [neglecting a factor 2]

$$\begin{aligned} S_I(\omega) &= S_I(\omega=0) - 2\hbar j M^{-1} \frac{(\omega = \gamma)^2}{(\omega = \gamma)^2 + M^2} \mathcal{A}_{ii} \\ &+ 2\hbar j \frac{(\omega = \gamma)^2}{(\omega = \gamma)^2 + M^2} \rho_{R,p}(\tau=0) \quad (E9) \end{aligned}$$

$$\begin{aligned} S_I(\omega=0) &= 2\hbar j M^{-1} \mathcal{A}_{ii} \frac{\hbar i}{(-e)} \rho_{ij} \\ &+ \tilde{\gamma}_R \rho_{22}^i - 4i\tilde{\gamma}_R \rho_{1,1}^i + \rho_{1,1}^i \end{aligned} \quad (E10)$$

The explicit expression for $S_I(\omega=0)$ is given in the main text.

These authors contributed equally to this work.

¹ D. J. W. Ineland and W. M. Itano, Phys. Rev. A 20, 1521 (1979).

² I. Martin, A. Shnirman, L. Tian, and P. Zoller, Phys. Rev. B 69, 125339 (2004).

³ P. Zhang, Y. D. Wang, and C. P. Sun, Phys. Rev. Lett.

95, 097204 (2005).

⁴ J. Hauss, A. Fedorov, C. Hutter, A. Shnirman, and G. Schon, Phys. Rev. Lett. 100, 037003 (2008).

⁵ K. Jaehne, K. Hammerer, and M. Wallquist, New J. Phys. 10, 095019 (2008).

⁶ Y. D. Wang, K. Semba, and H. Yamaguchi, New J. Phys.

- 10, 043015 (2008).
- ⁷ J. Q. You, Y.-X. Liu, and F. Nori, *Phys. Rev. Lett.* **100**, 047001 (2008).
 - ⁸ M. P. Blencowe, J. Imbers, and A. D. Armour, *New J. Phys.* **7**, 236 (2005).
 - ⁹ A. A. Clerk and S. Bennett, *New J. Phys.* **7**, 238 (2005).
 - ¹⁰ A. Naik, O. Buu, M. D. LaHaye, A. D. Armour, A. A. Clerk, M. P. Blencowe, K. C. Schwab, *Nature* **443**, 193 (2006).
 - ¹¹ I. Wilson-Rae, P. Zoller, and A. Imamoglu, *Phys. Rev. Lett.* **92**, 075507 (2004).
 - ¹² L. Tian and P. Zoller, *Phys. Rev. Lett.* **93**, 266403 (2004).
 - ¹³ C. H. Metzger and K. Karrai, *Nature* **432**, 1002 (2004).
 - ¹⁴ S. Gigan et al., *Nature* **444**, 67 (2006).
 - ¹⁵ O. Arcizet, P.-F. Cohadon, T. Briant, M. Pinard, and A. Heidmann, *Nature* **444**, 71 (2006).
 - ¹⁶ D. Kleckner and D. Bouwmeester, *Nature* **444**, 75 (2006).
 - ¹⁷ A. Schliesser, P. DelHaye, N. Nooshi, K. J. Vahala, and T. J. Kippenberg, *Phys. Rev. Lett.* **97**, 243905 (2006).
 - ¹⁸ T. Corbitt et al., *Phys. Rev. Lett.* **98**, 150802 (2007).
 - ¹⁹ J. D. Thompson, B. M. Zwickl, A. M. Jayich, F. Marquardt, S. M. Girvin, and J. G. E. Harris, *Nature* **452**, 72 (2008).
 - ²⁰ A. Schliesser, R. Riviere, G. Anetsberger, O. Arcizet, and T. J. Kippenberg, *Nature Physics* **4**, 415 (2008).
 - ²¹ S. Mancini, D. Vitali, and P. Tombesi, *Phys. Rev. Lett.* **80**, 688 (1998).
 - ²² D. Vitali, S. Mancini, L. R. Ibichini, and P. Tombesi, *Phys. Rev. A* **65**, 063803 (2002).
 - ²³ M. G. Rajar, S. Ashhab, J. R. Johansson, and F. Nori, *Phys. Rev. B* **78**, 035406 (2008).
 - ²⁴ M. Paternostro, S. Gigan, M. S. Kim, F. Blaser, H. R. Bohm, and M. Aspelmeyer, *New J. Phys.* **8**, 107 (2006).
 - ²⁵ I. Wilson-Rae, N. Nooshi, W. Zwerger, and T. J. Kippenberg, *Phys. Rev. Lett.* **99**, 093901 (2007).
 - ²⁶ F. Marquardt, J. P. Chen, A. A. Clerk, and S. M. Girvin, *Phys. Rev. Lett.* **99**, 093902 (2007).
 - ²⁷ M. Bhattacharya and P. Meystre, *Phys. Rev. Lett.* **99**, 073601 (2007).
 - ²⁸ C. Genes, D. Vitali, P. Tombesi, S. Gigan, and M. Aspelmeyer, *Phys. Rev. A* **77**, 033804 (2008).
 - ²⁹ A. Dantan, C. Genes, D. Vitali, and M. Pinard, *Phys. Rev. A* **77**, 011804 (R) (2008).
 - ³⁰ T. J. Kippenberg and K. J. Vahala, *Optics Express* **15**, 17172 (2007).
 - ³¹ F. Marquardt, A. A. Clerk, and S. M. Girvin, *arXiv:0803.1164*.
 - ³² D. J. Wineland et al., *arXiv:quant-ph/0606180*.
 - ³³ K. R. Brown, J. Britton, R. J. Epstein, J. Chiaverini, D. Leibfried, and D. J. Wineland, *Phys. Rev. Lett.* **99**, 137205 (2007).
 - ³⁴ F. Xue, Y. D. Wang, Y.-X. Liu, and F. Nori, *Phys. Rev. B* **76**, 205302 (2007).
 - ³⁵ M. D. LaHaye, O. Buu, B. Camarota, and K. C. Schwab, *Science* **304**, 74 (2004).
 - ³⁶ R. K. Nobel and A. N. Cleland, *Nature* **424**, 291 (2003).
 - ³⁷ N. E. Flowers-Jacobs, D. R. Schmidt, and K. W. Lehnert, *Phys. Rev. Lett.* **98**, 096804 (2007).
 - ³⁸ D. V. Averin and V. Ya. Aleshkin, *JETP Lett.* **50**, 367 (1989).
 - ³⁹ A. M. Aassen van den Brink, G. Schon, and L. J. Geerligs, *Phys. Rev. Lett.* **67**, 3030 (1991); A. M. van den Brink, A. A. Odintsov, P. A. Bobbert, and G. Schon, *Z. Phys. B* **85**, 459 (1991).
 - ⁴⁰ T. J. Harvey, D. A. Rodrigues, and A. D. Armour, *Phys. Rev. B* **78**, 024513 (2008).
 - ⁴¹ M.-S. Choi, R. Fazio, J. Siewert, and C. Bruder, *Europhys. Lett.* **53**, 251 (2001).
 - ⁴² Y. Nakamura, C. D. Chen, and J. S. Tsai, *Phys. Rev. B* **53**, 8234 (1996).
 - ⁴³ A. A. Clerk, *Proceedings of the NATO ASI New Directions in Mesoscopic Physics, Erice* (2002) [*arXiv:cond-mat/0301277v1*].
 - ⁴⁴ A. D. Armour, *Phys. Rev. B* **70**, 165315 (2004).
 - ⁴⁵ A. D. Armour, M. P. Blencowe, and Y. Zhang, *Phys. Rev. B* **69**, 125313 (2004).
 - ⁴⁶ D. A. Rodrigues and A. D. Armour, *New J. Phys.* **7**, 251 (2005).
 - ⁴⁷ D. A. Rodrigues and A. D. Armour, *Phys. Rev. B* **72**, 085324 (2005).
 - ⁴⁸ C. B. Doiron, W. Belzig, and C. Bruder, *Phys. Rev. B* **74**, 205336 (2006).
 - ⁴⁹ R. B. Lehoucq and D. C. Sorensen, *SIAM Journal on Matrix Analysis and Applications* **17**, 789 (1996).
 - ⁵⁰ O. Schenk and K. Gartner, *Future Generation Computer Systems* **20**, 475 (2004).
 - ⁵¹ O. Schenk and K. Gaertner, *Electron T Numer Ana* **23**, 158 (2006).
 - ⁵² C. Flindt, T. Novotny, and A.-P. Jauho, *Phys Rev B* **70**, 205334 (2004).
 - ⁵³ C. Flindt, T. Novotny, and A.-P. Jauho, *Europhys. Lett.* **69**, 475 (2005).
 - ⁵⁴ O. Usmani, Ya. M. Blanter, and Yu. V. Nazarov, *Phys. Rev. B* **75**, 195312 (2007).
 - ⁵⁵ A. Isacsson and T. Nord, *Europhys. Lett.* **66**, 708 (2004).
 - ⁵⁶ T. Novotny, A. Donarini, C. Flindt, and A.-P. Jauho, *Phys. Rev. Lett.* **92**, 248302 (2004).
 - ⁵⁷ F. Pistolesi and S. Labarthe, *Phys. Rev. B* **76**, 165317 (2007).
 - ⁵⁸ F. Pistolesi, *Phys. Rev. B* **69**, 245409 (2004).
 - ⁵⁹ A. A. Clerk, S. M. Girvin, A. K. Nguyen, and A. D. Stone, *Phys. Rev. Lett.* **89**, 176804 (2002).
 - ⁶⁰ A. N. Jordan and E. V. Sukhorukov, *Phys. Rev. Lett.* **93**, 260604 (2004).
 - ⁶¹ S. D. Bennett and A. A. Clerk, *Phys. Rev. B* **78**, 165328 (2008).
 - ⁶² D. A. Rodrigues (2008), *arXiv:0808.1169v1*.
 - ⁶³ C. W. Gardiner and P. Zoller, *Quantum Noise: A Handbook of Markovian and Non-Markovian Quantum Stochastic Methods with Applications to Quantum Optics*, Springer Series in Synergetics (Springer, Heidelberg, 2004), 3rd ed.
 - ⁶⁴ C. Flindt, T. Novotny, and A. Jauho, *Physica E* **29**, 411 (2005).
 - ⁶⁵ D. K. C. MacDonald, *Rep. Prog. Phys.* **12**, 56 (1949).
 - ⁶⁶ M.-S. Choi, F. Pastina, and R. Fazio, *Phys. Rev. B* **67**, 045105 (2003).
 - ⁶⁷ S. D. Bennett and A. A. Clerk, *Phys. Rev. B* **74**, 201301 (R) (2006).
 - ⁶⁸ Jian-Xin Zhu, Z. Nussinov, and A. V. Balatsky, *Phys. Rev. B* **73**, 064513 (2006).
 - ⁶⁹ An element D_{jk} of the matrix $D = (C^T A)$, with A a $2N_{\max} \times 2N_{\max}$ matrix, is therefore given by $D_{jk} = C_{ji} A_{kl}$ with $i = 4N_{\max}(j-1) + k$ and $l = 4N_{\max}(j-1) + 1$.